OPEN ACCESS Freely available online

PLoS one

Circulating Levels of Adiponectin, Leptin, Fetuin-A and Retinol-Binding Protein in Patients with Tuberculosis: Markers of Metabolism and Inflammation

Naoto Keicho[1]*, Ikumi Matsushita[1], Takahiro Tanaka[1], Takuro Shimbo[2], Nguyen Thi Le Hang[3], Shinsaku Sakurada[1], Nobuyuki Kobayashi[4], Minako Hijikata[1], Pham Huu Thuong[5], Luu Thi Lien[5]

1 Department of Respiratory Diseases, Research Institute, National Center for Global Health and Medicine, Tokyo, Japan, **2** Department of Clinical Research and Informatics, International Clinical Research Center, National Center for Global Health and Medicine, Tokyo, Japan, **3** National Center for Global Health and Medicine–Bach Mai Hospital Medical Collaboration Center, Hanoi, Viet Nam, **4** Department of Respiratory Medicine, National Center for Global Health and Medicine, Tokyo, Japan, **5** Hanoi Lung Hospital, Hanoi, Viet Nam

Abstract

Background: Wasting is known as a prominent feature of tuberculosis (TB). To monitor the disease state, markers of metabolism and inflammation are potentially useful. We thus analyzed two major adipokines, adiponectin and leptin, and two other metabolic markers, fetuin-A and retinol-binding protein 4 (RBP4).

Methods: The plasma levels of these markers were measured using enzyme-linked immunosorbent assays in 84 apparently healthy individuals (=no-symptom group) and 46 patients with active pulmonary TB around the time of treatment, including at the midpoint evaluation (=active-disease group) and compared them with body mass index (BMI), C-reactive protein (CRP), chest radiographs and TB-antigen specific response by interferon-γ release assay (IGRA).

Results: In the no-symptom group, adiponectin and leptin showed negative and positive correlation with BMI respectively. In the active-disease group, at the time of diagnosis, leptin, fetuin-A and RBP4 levels were lower than in the no-symptom group [adjusted means 2.01 versus 4.50 ng/ml, $P<0.0001$; 185.58 versus 252.27 μg/ml, $P<0.0001$; 23.88 versus 43.79 μg/ml, $P<0.0001$, respectively]. High adiponectin and low leptin levels were associated with large infiltrates on chest radiographs even after adjustment for BMI and other covariates ($P=0.0033$ and $P=0.0020$). During treatment, adiponectin levels increased further and then decreased. Leptin levels remained low. Initial low levels of fetuin-A and RBP4 almost returned to the normal reference range in concert with reduced CRP.

Conclusions: Our data and recent literature suggest that low fat store and underlying inflammation may regulate these metabolic markers in TB in a different way. Decreased leptin, increased adiponectin, or this ratio may be a promising marker for severity of the disease independent of BMI. We should further investigate pathological roles of the balance between these adipokines.

Citation: Keicho N, Matsushita I, Tanaka T, Shimbo T, Hang NTL, et al. (2012) Circulating Levels of Adiponectin, Leptin, Fetuin-A and Retinol-Binding Protein in Patients with Tuberculosis: Markers of Metabolism and Inflammation. PLoS ONE 7(6): e38703. doi:10.1371/journal.pone.0038703

Editor: Pere-Joan Cardona, Fundació Institut d'Investigació en Ciències de la Salut Germans Trias i Pujol. Universitat Autònoma de Barcelona. CIBERES, Spain

Received January 19, 2012; **Accepted** May 9, 2012; **Published** June 7, 2012

Funding: This work was supported by a grant from the Program of Japan Initiative for Global Research Network on Infectious Diseases, MEXT, Japan. The funders had no role in study design, data collection and analysis, decision to publish, or preparation of the manuscript.

Competing Interests: The authors have declared that no competing interests exist.

* E-mail: nkeicho-tky@umin.ac.jp

Introduction

Tuberculosis (TB) is a major infectious cause of death around the world, with most of the 1.5 million deaths per year attributable to the disease occurring in developing countries. Negative energy balance in chronic inflammation has been recognized as a prominent feature of TB and one of the major obstacles to manage the patients [1,2]. Recent emergence of drug resistant TB is assumed to be driven by poorly implemented drug regimens, but malnutrition as well as HIV co-infection might worsen the condition: Inflammatory responses evoked by infection increase the demand for anabolic energy, leading to a synergistic vicious circle and further deterioration of the clinical condition [3].

It is generally believed that undernourishment diminishes protective immunity against *Mycobacterium tuberculosis*. [4]. A series of animal experiments, particularly aerosol-infected guinea pig models have demonstrated that chronic protein-energy malnutrition reduces secretion of T-helper 1 (Th1) cytokines [5]. It is rapidly reversed with alimentary supplement, indicating a pivotal role of nutrition, although it remains unclear what the optimal nutritional interventions are for improving the human disease in an effective manner [4].

On the other hand, in many countries today, rapid industrialization and urbanization are accompanied by changing patterns of diet and physical activity and this results in overnutrition [6]. Consequently, a combination of these two unfavor-

Table 1. Characteristics of study population.

	no-symptom group (N = 84)	active-disease group (N = 46)	*P* values
Male/Female (n)	41/43	42/4	<0.0001
Age (year)*	40.0 (28.1–48.6)	47.2 (34.7–55.0)	0.0064
BMI (kg/m^2)*	21.8 (20.0–23.7)	18.3 (17.1–19.5)	<0.0001
BCG history (yes/no/unknown)	33/28/23	10/3/33	<0.0001
positive/negative results of IGRA (n)	55/29	41/4**	0.0015

*Median and 25-to-75 percentiles in parenthesis are shown.
**One indeterminate case is not shown here.
doi:10.1371/journal.pone.0038703.t001

able conditions, a slow decline of infectious diseases associated with undernutrition and a rapid increase in obesity and diabetes are a serious double burden to public health and clinical medicine in resource limited settings [7].

Mainly in studies carried out in industrialized countries, fat-cell-derived hormones/cytokines designated as adipokines and relevant mediators have been investigated extensively and proposed as markers of obesity and diabetes [8]. Of these adipokines, adiponectin is a unique insulin sensitizer with atheroprotective role [9,10]. Plasma levels of adiponectin are inversely correlated with body weight and visceral fat mass [11,12]. Leptin is another major adipokine in proportion to fat stores [13,14] and one of the key mediators of energy metabolism [2] Even mild weight loss induced by dietary restriction is known to reduce leptin levels [11]. These markers supposedly shift towards the opposite in lean patients with wasting diseases. However, the significance of these metabolic markers in chronic infectious diseases like TB has not been fully understood [2].

We have recently conducted a proteomic research and demonstrated that plasma levels of fetuin-A and retinol-binding protein 4 (RBP4), also closely linked to the metabolic and inflammatory state, were significantly lower in patients with active pulmonary TB than in control subjects [15]. Fetuin-A, also known as α2-Heremans-Schmid glycoprotein, is an abundant plasma component of hepatic origin [16] and a negative regulator of insulin signaling [17,18]. Elevation of plasma fetuin-A is strongly associated with atherogenic lipid profile as well as fatty liver in obese patients [18]. Lipid components in the liver presumably upregulate fetuin-A expression, which may in turn repress adiponectin and impair adipocyte function [19,20]. Fetuin-A is also downregulated in acute inflammation as a negative acute-phase protein [21]. RBP4, synthesized in the liver and adipose tissue, has recently been identified as another adipokine involved in the development of insulin resistance [22]. In humans, similar to leptin, circulating RBP4 levels are high in obesity and decreased after calorie-restriction induced weight loss [11,23]. RBP4 is also known as a specific transporter protein for retinol (vitamin A) and can be used to assess the short-term fluctuation of nutritional states as a rapid turnover protein [24].

Alteration of the circulating levels of these markers should be investigated in TB, since they are expected to provide a basis of a critical link among nutritional status, metabolism and immunity of the disease, and hopefully to consider efficient nutritional interventions. In the present study, we thus measured circulating adiponectin and leptin in addition to fetuin-A and RBP4 levels in patients with active pulmonary TB versus apparently healthy individuals and compared the levels with body mass index (BMI), a simple estimate of adiposity [25] and C-reactive protein (CRP),

Table 2. Correlation of tested marker levels with BMI, CRP and IGRA values in each of the no-symptom and active-disease groups.

	no-symptom group (N = 84)			active-disease group (N = 46)		
	Pearson's *r* (*P* values)[a]			Pearson's *r* (*P* values)[a]		
Variable	by BMI (kg/m^2)	by CRP (μg/ml)	by IFN-γ (IU/ml)[b]	by BMI (kg/m^2)	by CRP (μg/ml)	by IFN-γ (IU/ml)[b]
Adiponectin (μg/ml)	−0.4530	−0.2892	−0.2254	−0.4421	0.1477	−0.1092
	(<0.0001)*	(0.0076)	(0.0393)	(0.0021)	(0.3274)	(0.4700)
Leptin (ng/ml)	0.4518	0.1694	0.1179	0.2771	−0.0918	0.3568
	(<0.0001)*	(0.1234)	(0.2855)	(0.0623)	(0.5442)	(0.0149)
Leptin/adiponectin ratio	0.5820	0.2793	0.2067	0.4901	−0.1633	0.2804
	(<0.0001)*	(0.0101)	(0.0592)	(0.0005)*	(0.2783)	(0.0591)
Fetuin-A (μg/ml)	0.0309	0.0415	0.0322	0.1243	−0.1833	0.2402
	(0.7805)	(0.7079)	(0.7714)	(0.4105)	(0.2226)	(0.1078)
RBP4 (μg/ml)	0.1605	−0.0213	0.0716	0.1535	−0.3018	−0.0916
	(0.1447)	(0.8475)	(0.5173)	(0.3085)	(0.0415)	(0.5448)

[a]Pearson's correlation coefficients with *P* values were calculated. Plasma concentrations were analyzed after logarithmic transformation.
[b]TB-antigen stimulated IFN-γ response
*Statistically significant when the significance level is set as $P<0.002$ based on the Bonferrroni correction.
doi:10.1371/journal.pone.0038703.t002

Table 3. BMI, CRP and tested marker levels in IGRA-positive and -negative subgroups in the no-symptom group.

	IGRA-negative (N = 29)		IGRA-positive (N = 55)		
marker	adjusted mean[a]	(95%CI)	adjusted mean[a]	(95%CI)	*P* values (ANCOVA)
BMI (kg/m^2)	21.52	(20.58–22.46)	21.48	(20.74–22.22)	0.9392
CRP (μg/ml)	1.12	(0.60–2.08)	1.30	(0.80–2.12)	0.6663
Adiponectin (μg/ml)	7.19	(5.67–9.11)	6.39	(5.30–7.70)	0.3792
Leptin (ng/ml)	4.50	(3.34–6.05)	4.38	(3.47–5.54)	0.8783
Leptin/adiponectin ratio	0.63	(0.40–0.97)	0.69	(0.49–0.97)	0.7080
Fetuin-A (μg/ml)	234.22	(212.40–258.29)	263.88	(244.26–285.06)	0.0333
RBP4 (μg/ml)	39.64	(32.28–48.69)	42.88	(36.45–50.43)	0.4997

[a]Estimated means of plasma concentrations were compared after logarithmic transformation, being adjusted for gender and age as covariates. The data shown are transformed back to the original unit.
No *P* values were statistically significant when the significance level is set as $P<0.007$ based on the Bonferrroni correction.
doi:10.1371/journal.pone.0038703.t003

a representative positive acute phase protein [26]. We further characterized their relationship with disease severity and alterations during the course of treatment.

Methods

Study design

We randomly selected and used plasma samples and demographic information in 46 patients with active pulmonary TB (= active-disease group) without treatment history as a biomarker sub-study of a large cohort study [27]. All patients entered the study from July 2007 to March 2009. Diagnosis of active pulmonary TB was made clinically and radiologically and confirmed bacteriologically in Hanoi Lung Hospital. A sputum smear test showed positive results in all of the patients in the active disease group and all of them completed anti-TB treatment following the national standard regimen, 2 months of streptomycin, isoniazid, rifampicin, and pyrazinamide followed by 6 months of isoniazid and ethambutol (2SHRZ/6HE).

Chest radiographs were taken at the time of diagnosis and interpreted by two readers independently in a blind manner. The presence of cavitary lesions and the number of lung zones (zero to six corresponding to the upper, middle, and lower fields on the right and left sides of the lung) affected by infiltrates were recorded [28]. HIV status was examined before starting anti-TB treatment. The proportion of HIV co-infection is less than 10% in this study area and those with HIV positive were excluded from the drawing up of this sub-study.

As a reference, we also measured plasma samples derived from 84 apparently healthy men and women who may have chances of direct or indirect contacts with TB patients as health care staff (= no-symptom group). All participants were tested for TB-antigen specific interferon-γ response by the commercially available enzyme-linked immunosorbent assay (ELISA)-based interferon-γ release assay (IGRA), QuantiFERON-TB Gold In-Tube™ (Cellestis, Victoria, Australia). In the no-symptom group, IGRA-positive individuals suspected of latent TB infection were recommended to take chest radiography and to confirm there were no active pulmonary lesions. Subsequently a chance of receiving isoniazid prophylactic therapy was given. The protocol was approved by ethical committees of the Ministry of Health, Viet Nam and National Center for Global Health and Medicine, Japan respectively and written informed consent was obtained from each participant.

Table 4. BMI, CRP and tested marker levels in the no-symptom and active-disease groups after adjustment for gender and age.

	no-symptom group (N = 84)		active-disease group (N = 46)		
marker	adjusted mean[a]	(95%CI)	adjusted mean[a]	(95%CI)	*P* values (ANCOVA)
BMI (kg/m^2)	21.68	(21.06–22.30)	17.65	(16.66–18.65)	<0.0001*
CRP (μg/ml)	1.22	(0.86–1.74)	36.88	(20.94–64.94)	<0.0001*
Adiponectin (μg/ml)	6.82	(5.73–8.12)	9.29	(7.02–12.30)	0.0136
Leptin (ng/ml)	4.50	(3.78–5.35)	2.01	(1.52–2.66)	<0.0001*
Leptin/adiponectin ratio	0.66	(0.50–0.88)	0.22	(0.14–0.34)	<0.0001*
Fetuin-A (μg/ml)	252.27	(234.55–271.33)	185.58	(165.07–208.64)	<0.0001*
RBP4 (μg/ml)	43.79	(38.09–50.34)	23.88	(19.08–29.88)	<0.0001*

[a]Estimated means of plasma concentrations were compared after logarithmic transformation, being adjusted for gender and age as covariates. The data shown are transformed back to the original unit.
*Statistically significant when the significance level is set as $P<0.007$ based on the Bonferrroni correction.
doi:10.1371/journal.pone.0038703.t004

Table 5. CRP and tested marker levels in the no-symptom and active-disease groups after adjustment for gender, age and BMI.

	no-symptom group (N = 84)		active-disease group (N = 46)		
marker	adjusted mean[a]	(95%CI)	adjusted mean[a]	(95%CI)	*P* values (ANCOVA)
CRP (μg/ml)	1.11	(0.77–1.60)	47.80	(25.36–90.09)	<0.0001*
Adiponectin (μg/ml)	7.80	(6.63–9.19)	6.39	(4.81–8.49)	0.1671
Leptin (ng/ml)	3.77	(3.26–4.37)	3.28	(2.54–4.24)	0.2790
Leptin/adiponectin ratio	0.48	(0.38–0.61)	0.51	(0.35–0.76)	0.7704
Fetuin-A (μg/ml)	248.04	(229.95–267.57)	194.46	(170.48–221.80)	0.0004*
RBP4 (μg/ml)	42.90	(37.08–49.63)	25.27	(19.62–32.55)	0.0001*

[a]Estimated means of plasma concentrations were compared after logarithmic transformation, being adjusted for gender, age and BMI as covariates. The data shown are transformed back to the original unit.
*Statistically significant when the significance level is set as $P<0.008$ based on the Bonferrroni correction.
doi:10.1371/journal.pone.0038703.t005

Measurements of markers of metabolism and inflammation

Immediately after making the diagnosis of active TB disease, heparinized blood samples were drawn for IGRA before starting anti-TB treatment (0 month) and the remaining plasma without mixing any stimulants was reserved in a −80°C freezer until measurement. Samples were collected twice again, after the initial phase of treatment (2 months) and at the end of treatment (7 months) in the active disease group. This study was originally intended to identify a variety of biomarkers associated with TB phenotypes [15] and the participants were not obliged to keep fasting. The blood was collected in the daytime between 8 am and 4 pm at the outpatient clinic to avoid interference in dosing schedule of anti-TB drugs.

The AssayMax Human C-Reactive Protein ELISA kit was used for detection of human c-reactive protein (CRP) in plasma (Assaypro LLC. St. Charles, MO, USA). The minimum detectable dose was less than 0.25 ng/ml. The Quantikine® Human Total Adiponectin/Acrp30 Immunoassay kit was used to detect total (low, middle and high molecular weight) human adiponectin in plasma (R&D Systems, Inc.; Minneapolis, MN, USA). The mean minimum detectable dose was 0.246 ng/ml. The Quantikine® Human Leptin Immunoassay kit was used to detect human leptin in plasma (R&D Systems, Inc.). The mean minimum detectable dose was 7.8 pg/ml. The AHSG ELISA kit was used to detect fetuin-A in plasma (BioVender Laboratory Medicine Inc.; Modrice, Czech Republic). The detection limit was 0.35 ng/ml. A competitive ELISA for quantitative determination of RBP4 in human plasma was also applied (AdipoGen Inc.; Seoul, Korea) and the detection limit was 1 ng/ml. All were performed according to the manufacturer's instructions. Differences in measured concentrations between EDTA plasma samples as reference and these heparin samples were within a range of variation generally accepted in ELISA (coefficient of variance <15%) (data not shown)

Statistical analysis

Plasma protein levels were served for subsequent statistical analysis after logarithmic transformation of the measurements to minimize distortion of the data distribution. Means of demographic data between two groups were compared by analysis of variance (ANOVA) after testing for equal variances and

Table 6. BMI, CRP and tested marker levels in patients with small and large infiltrates on chest radiographs after adjustment for gender and age.

	small infiltrates[a] (N = 22)		large infiltrates[a] (N = 23)		
marker	adjusted mean[b]	(95%CI)	adjusted mean[b]	(95%CI)	*P* values (ANCOVA)
BMI (kg/m^2)	18.73	(16.74–20.71)	18.11	(15.95–20.27)	0.3065
CRP (μg/ml)	26.14	(12.63–54.10)	35.92	(16.29–79.21)	0.1520
Adiponectin (μg/ml)	10.28	(5.38–19.66)	18.83	(9.31–38.11)	0.0033*
Leptin (ng/ml)	2.42	(1.64–3.57)	1.65	(1.08–2.52)	0.0020*
Leptin/adiponectin ratio	0.24	(0.11–0.52)	0.09	(0.04–0.21)	0.0002*
Fetuin-A (μg/ml)	201.97	(149.87–272.18)	184.68	(133.52–255.46)	0.3222
RBP4 (μg/ml)	36.14	(21.76–60.03)	31.56	(18.17–54.79)	0.3770
IFN-γ (IU/ml)[c]	11.04	(2.13–57.16)	5.80	(0.97–34.82)	0.2039

[a]Small infiltrates = less than 3 of 6 zones in the lung affected, large infiltrates = 3 or more than 3 of 6 zones affected
[b]Estimated means of plasma concentrations were compared after logarithmic transformation, being adjusted for gender and age as covariates. The data shown are transformed back to the original unit.
[c]TB-antigen stimulated IFN-γ response
*Statistically significant when the significance level is set as $P<0.006$ based on the Bonferrroni correction.
doi:10.1371/journal.pone.0038703.t006

Table 7. CRP and tested marker levels in patients with small and large infiltrates on chest radiographs after adjustment for gender, age and BMI.

	small infiltrates[a] (N = 22)		large infiltrates[a] (N = 23)		
marker	**adjusted mean[b]**	**(95%CI)**	**adjusted mean[b]**	**(95%CI)**	***P* values (ANCOVA)**
CRP (μg/ml)	26.59	(12.78–55.28)	35.50	(16.02–78.63)	0.1991
Adiponectin (μg/ml)	10.84	(6.01–19.53)	18.15	(9.57–34.40)	0.0061*
Leptin (ng/ml)	2.37	(1.63–3.47)	1.67	(1.11–2.52)	0.0040*
Leptin/adiponectin ratio	0.22	(0.11–0.44)	0.09	(0.04–0.20)	0.0002*
Fetuin-A (μg/ml)	200.77	(148.59–271.28)	185.46	(133.74–257.18)	0.3886
RBP4 (μg/ml)	35.69	(21.43–59.46)	31.83	(18.29–55.42)	0.4626
IFN-γ (IU/ml)[c]	11.41	(2.17–59.90)	5.68	(0.94–34.53)	0.1760

[a]Small infiltrates = less than 3 of 6 zones in the lung affected, large infiltrates = 3 or more than 3 of 6 zones affected
[b]Estimated means of plasma concentrations were compared after logarithmic transformation, being adjusted for gender, age and BMI as covariates. The data shown are transformed back to the original unit.
[c]TB-antigen stimulated IFN-γ response
*Statistically significant when the significance level is set as $P<0.007$ based on the Bonferrroni correction.
doi:10.1371/journal.pone.0038703.t007

proportions between two groups were compared by the chi-squared test. Since it is well known that levels of adipokines such as leptin are influenced by gender and age, measurements of protein markers in any two groups were compared by analysis of covariance (ANCOVA) to allow for the covariates. The relationship between markers and other parameters were assessed by Pearson's correlation coefficients. Overall alterations of the measurements at three time points were initially analyzed by repeated-measures ANOVA and only when statistically significant, post-hoc comparisons were proceeded to: Difference of values between two time points was assessed by the paired-T test, under normal approximation based on the central limit theorem. P values<0.05 were considered to be statistically significant in general. When the Bonferroni correction was applied, however, a level of statistical significance was set as $0.05/n$ (n = the number of comparisons). Statistical analysis was performed using Stata version 11 (StataCorp, College Station, TX, USA).

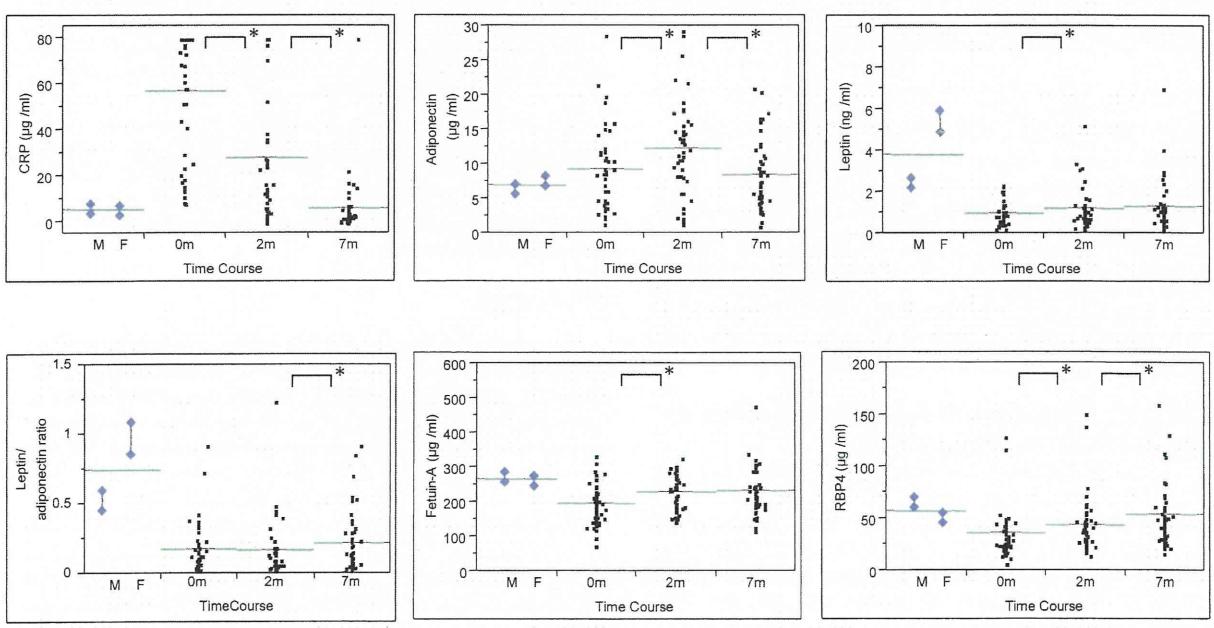

Figure 1. CRP and tested marker levels in patients with active TB before (0 month), during (2 months) and at the end (7 months) of anti-TB treatment (N = 46). Vertical bars with diamonds on the left side (M and F) indicate reference values, means ± SEM of the values in men (N = 41) and women (N = 43) of the no-symptom group. A horizontal bar indicates the grand mean of the values in each condition. * indicates $P<0.05$ by paired comparison between 0 month and 2 months. When significant, 2 months and 7 months were also compared.
doi:10.1371/journal.pone.0038703.g001

Results

Characteristics of study population

The no-symptom group consisted of 84 apparently healthy individuals, whose blood samples were used to obtain the standard values of markers in the study population. This group includes an approximately equal number of men and women with median age of 40, and more than half of the individuals had latent TB infection diagnosed by the IGRA method (Table 1). The active-disease group members were 46 patients with smear-positive active pulmonary TB. The majority of the patients were male with low body mass index (BMI<18.5 kg/m^2) and the median age was 47, slightly older than in the non-symptom group.

Correlation of adiponectin, leptin, fetuin-A and RBP4 levels with BMI, CRP and IGRA values in the no-symptom and active-disease groups

Correlation coefficients (r) were calculated in the no-symptom and active-disease groups respectively (Table 2). Adiponectin and leptin showed negative and positive correlations with BMI respectively in the no-symptom group ($r=-0.4530$, $P<0.0001$; $r=0.4518$, $P<0.0001$). Leptin/adiponectin ratio showed a positive correlation with BMI in the active-disease group ($r=0.4901$, $P=0.0005$) as well as in the no-symptom group ($r=0.5820$, $P<0.0001$). These correlations were statistically significant even after Bonferroni correction for multiple comparisons. The other possible correlations including a pair of leptin and TB-antigen stimulated IFN-γ response did not reach significant levels in this study, when Bonferroni correction was applied.

Pairwise correlations between four tested markers

Pairwise correlation coefficients (r) between four tested metabolic markers were further calculated in the no-symptom and active-disease groups respectively (Table S1). A significant correlation was found only between fetuin-A and RBP4 levels ($r=0.4007$, $P=0.0058$) in the active disease group.

Adiponectin, leptin, fetuin-A and RBP4 levels with IGRA-positive and -negative subgroups in the no-symptom group

IGRA-positive values higher than the cutoff value, 0.35 IU/ml are regarded as latent TB infection after active disease is ruled out. We thus categorized the no-symptom group into IGRA-positive and -negative subgroups and compared plasma concentrations of the above markers. However, none of the marker levels including fetuin-A were significantly different between IGRA-positive and -negative subgroups after adjustment for gender and age, when considering the number of comparisons (Table 3).

Adiponectin, leptin, fetuin-A and RBP4 levels in the no-symptom and active-disease groups

The active-disease group had significantly low BMI and very high CRP levels at the time of diagnosis, when assessed by using ANCOVA with adjusted means (Table 4). In the disease group, leptin, leptin/adiponectin ratio, fetuin-A and RBP4 levels were remarkably lower than in the no-symptom group ($P<0.0001$ respectively) after adjustment for gender and age and these differences were statistically significant even after Bonferroni correction (Table 4).

Since BMI was strongly correlated with some of the adipokine values as shown in Table 2, we further analyzed levels of the four markers after adjustment for BMI as well as gender and age. Consequently, adiponectin and leptin levels were not significantly different between the two groups any more, whereas fetuin-A and RBP4 levels remained significant ($P=0.0004$ and $P=0.0001$) (Table 5)

Adiponectin, leptin, fetuin-A and RBP4 levels in patients with mild and severe disease

At the time of diagnosis, severity of the disease was assessed by spread of infiltrates on chest radiographs (Table 6). Small infiltrates affecting less than 3 of the 6 lung zones and large ones affecting more, categorized the patients into two subgroups (= mild and severe disease) half-and-half.

After adjustment for gender and age, adiponectin levels were higher and leptin levels were lower in patients with large infiltrates than in those with small infiltrates ($P=0.0033$ and $P=0.0020$). Interestingly, differences in the levels of these two adipokines between small and large infiltrates were significant respectively ($P=0.0061$ and $P=0.0040$), even after adjustment for BMI as well as gender and age (Table 7). Leptin/adiponectin ratio was lower, or adiponectin/leptin ratio was higher, in patients with large infiltrates than in those with small infiltrates independent of BMI ($P=0.0002$). None of the markers were associated with the presence of cavity on the chest radiographs (data not shown).

Adiponectin, leptin, fetuin-A and RBP4 levels in patients with active TB before, during and at the end of anti-TB treatment

Figure 1 shows plasma values at the time points before (0 month), during (2 months) and at the end (7 months) of anti-TB treatment. Mean values in men (N = 41) and women (N = 43) of the no-symptom group are shown as a reference, in which gender difference was observed in leptin levels and leptin/adiponectin ratio ($P<0.0001$).

Overall differences of the measurements during anti-TB treatment in all of these four markers were statistically significant by repeated-measures ANOVA ($P<0.01$). Post-hoc analysis showed that adiponectin levels increased transiently ($P=0.0004$; 0 month vs. 2 months) and then decreased close to the reference range by the end of treatment ($P<0.0001$; 2 months vs. 7 months). Leptin levels remained low throughout the treatment course, though gradually elevated ($P=0.0226$; 0 month vs. 2 months). Initial low levels of fetuin-A and RBP4 significantly improved during treatment ($P=0.0001$ and $P=0.0016$; 0 month vs. 2 months), almost reaching the reference range by the end in concert with reduced CRP levels.

Discussion

We assessed the clinical significance of four metabolic markers, adiponectin, leptin, fetuin-A and RBP4 in patients with active TB, analyzing them in relation to classical nutritional and inflammatory parameters, BMI and CRP, severity of disease and treatment course. BMI is known to be lower in patients with active TB than in control subjects [1,2]. After effective treatment, weight often increases but patients may remain underweight [11].

Plasma levels of adiponectin were inversely correlated with BMI in concordance with previous results [11,12]. The adiponectin levels tended to be elevated in the active-disease group characterized by low BMI, though it did not reach significant levels, which was also shown by others [29]. Interestingly in our study, adiponectin levels were significantly higher in severe disease with extensive pulmonary lesions than in mild disease, even after adjustment for BMI. Adiponectin as a modulator of inflammation in a variety of diseases has recently been highlighted [30]. For instance, in critically ill patients, adiponectin levels appear to be

transiently suppressed at the initial phase and then gradually elevated at the recovery phase [31,32]. The plasma concentrations in patients with active TB were further increased after starting treatment and then decreased close to the reference range by the end of treatment. Elevated adiponectin levels in chronic inflammatory diseases may be explained by compensatory response to the underlying disease as well as concomitant low body fat mass, which is postulated by others [33,34]. A study designed to measure alteration of adiponectin and BMI simultaneously throughout the treatment period would be able to characterize it further.

In most recent reports, leptin levels are low in TB [29,35–38], though other earlier or smaller studies have shown conflicting results [39–42]. In the present study, using a commercial ELISA, significantly lower levels of leptin were demonstrated in patients with active TB, which could be mostly explained by marked undernutrition in our disease population. Within the active-disease group, however, correlation between leptin and BMI was less clear. BMI-independent regulation of plasma leptin concentrations should also be taken into consideration in TB at least in part [13,37]. This idea is also supported by an *ex vivo* study by others demonstrating that continuous exposure of IL-1 or TNF-α provides a signal to downregulate leptin in human adipose tissue [43], though acute inflammation such as sepsis may rather upregulate circulating leptin levels transiently [44–46]. In addition to relatively high levels of adiponectin, low levels of leptin were observed in patients with large infiltrates, even after adjustment for BMI. This is concordant with a recent study showing that leptin levels were low in severe TB disease [29]. We have further demonstrated that low leptin/adiponectin ratio, or high adiponectin/leptin ratio is characteristic to severe TB disease in this study. This ratio was originally proposed as an atherogenic index indicating a balance between the two markers bearing apparently opposite functions in inflammation [47]. Our findings support the idea that suppressed production of leptin may be detrimental to host defense against TB by virtue of impairment of Th1 cell-mediated immunity [13,29,48]. After starting treatment, leptin levels were slightly elevated, but remained low during the treatment period. This is also compatible with reports made by others [37,38], although the mechanism remains unknown. Long-lasting low levels of leptin may be attributed to individual predisposition to TB or delayed recovery from wasting disease.

In our study, fetuin-A levels were considerably low in TB even after adjustment for BMI. Soon after starting treatment, the levels were increased in inverse proportion to the decrease in CRP. In TB, fetuin-A may be downregulated by at least dual mechanisms, strongly mediated by underlying inflammation [21] and partly controlled by depleted liver fat due to wasting or malnutrition [18]. Low fetuin-A levels may also result in impairment of macrophage function to kill the pathogen and ectopic calcification possibly in TB lesions [49,50].

RBP4 levels were also low in TB even after adjustment for BMI. Throughout the treatment course, the levels were gradually elevated close to the reference range inversely with the decrease in CRP. These findings are supported by a recent report demonstrating that RBP4 rapidly decreases during acute inflammation, possibly acting as a negative acute phase reactant, similar to fetuin-A, albumin and prealbumin [21,51,52]. This may partly explain a close positive correlation with fetuin-A demonstrated in the active-disease group. In addition to dual regulation of RBP4 by underlying inflammation and low body fat mass, reduced renal function is also known to cause retention of the circulating levels, such that further caution is needed to interpret RBP4 measurement in disease state [53].

Our study has several limitations. Firstly, many types of nutrients including micronutrients are essential to the human body but the potential interplay between each component of nutrients was not within our scope at that time. Secondly, since change of BMI was not measured during treatment, direct comparison of improved BMI with the corresponding marker levels was not possible. Thirdly, blood was collected during the daytime without enforced fasting. Although, of course, this increases the variance of measurements, it can be inferred that daytime variations on circulating adipokines and leptin [54] are not as large as to seriously affect conclusive results of comparisons within and between groups in this study. Finally, computer tomography, which has advantages over chest radiography as an imaging tool, was not available in our setting.

Overall, our data and recent literature would suggest that all of the four markers tested are controlled partly by low fat store and partly by inflammation in TB but their regulatory mechanisms are more or less different and interactions with other relevant factors including insulin sensitivity and cellular immunity are worth further investigation. In particular, leptin, adiponectin and their ratio may be promising markers for severity of the wasting disease. Since nutritional intervention has a potential to improve prognosis of intractable TB such as HIV co-infection and MDR-TB, large-scale prospective studies using selected biomarkers to investigate metabolic contributors to disease phenotype are desired. The more fully we understand the mechanisms linking diet, health, and disease, the more effective will be our ability to design optimal interventions.

Supporting Information

Table S1 Pairwise correlations between four tested markers.
(DOC)

Acknowledgments

We thank Tokie Totsu and Fumi Toshioka for their technical assistance. The authors thank Kazuko Tanabe D.V.M. and Mr. John Crosskey for their critical reading of this manuscript.

Author Contributions

Conceived and designed the experiments: N. Keicho IM TT N. Kobayashi SS. Performed the experiments: IM. Analyzed the data: N. Keicho IM NTLH TS. Contributed reagents/materials/analysis tools: IM TT NTLH SS MH PHT LTL. Wrote the paper: N. Keicho.

References

1. Tverdal A (1986) Body mass index and incidence of tuberculosis. Eur J Respir Dis 69: 355–362.
2. Schaible UE, Kaufmann SH (2007) Malnutrition and infection: complex mechanisms and global impacts. PLoS Med 4: e115.
3. Prentice AM, Gershwin ME, Schaible UE, Keusch GT, Victora CG, et al. (2008) New challenges in studying nutrition-disease interactions in the developing world. J Clin Invest 118: 1322–1329.
4. Cegielski JP, McMurray DN (2004) The relationship between malnutrition and tuberculosis: evidence from studies in humans and experimental animals. Int J Tuberc Lung Dis 8: 286–298.
5. Dai G, McMurray DN (1998) Altered cytokine production and impaired antimycobacterial immunity in protein-malnourished guinea pigs. Infect Immun 66: 3562–3568.
6. Leung CC, Lam TH, Chan WM, Yew WW, Ho KS, et al. (2007) Lower risk of tuberculosis in obesity. Arch Intern Med 167: 1297–1304.
7. Dooley KE, Chaisson RE (2009) Tuberculosis and diabetes mellitus: convergence of two epidemics. Lancet Infect Dis 9: 737–746.
8. Musaad S, Haynes EN (2007) Biomarkers of obesity and subsequent cardiovascular events. Epidemiol Rev 29: 98–114.

9. Yang WS, Lee WJ, Funahashi T, Tanaka S, Matsuzawa Y, et al. (2001) Weight reduction increases plasma levels of an adipose-derived anti-inflammatory protein, adiponectin. J Clin Endocrinol Metab 86: 3815–3819.
10. Pitombo C, Araújo EP, De Souza CT, Pareja JC, Geloneze B, et al. (2006) Amelioration of diet-induced diabetes mellitus by removal of visceral fat. J Endocrinol 191: 699–706.
11. Klempel MC, Varady KA (2011) Reliability of leptin, but not adiponectin, as a biomarker for diet-induced weight loss in humans. Nutr Rev 69: 145–154.
12. Kuo SM, Halpern MM (2011) Lack of association between body mass index and plasma adiponectin levels in healthy adults. Int J Obes (Lond) 35: 1487–1494.
13. Malli F, Papaioannou AI, Gourgoulianis KI, Daniil Z (2010) The role of leptin in the respiratory system: an overview. Respir Res 11: 152.
14. Klimcakova E, Kovacikova M, Stich V, Langin D (2010) Adipokines and dietary interventions in human obesity. Obes Rev 11: 446–456.
15. Tanaka T, Sakurada S, Kano K, Takahashi E, Yasuda K, et al. (2011) Identification of tuberculosis-associated proteins in whole blood supernatant. BMC Infect Dis 11: 71.
16. Denecke B, Gräber S, Schäfer C, Heiss A, Wöltje M, et al. (2003) Tissue distribution and activity testing suggest a similar but not identical function of fetuin-B and fetuin-A. Biochem J 376: 135–145.
17. Mori K, Emoto M, Yokoyama H, Araki T, Teramura M, et al. (2006) Association of serum fetuin-A with insulin resistance in type 2 diabetic and nondiabetic subjects. Diabetes Care 29: 468.
18. Stefan N, Hennige AM, Staiger H, Machann J, Schick F, et al. (2006) Alpha2-Heremans-Schmid glycoprotein/fetuin-A is associated with insulin resistance and fat accumulation in the liver in humans. Diabetes Care 29: 853–857.
19. Hennige AM, Staiger H, Wicke C, Machicao F, Fritsche A, et al. (2008) Fetuin-A induces cytokine expression and suppresses adiponectin production. PLoS One 3: e1765.
20. Dasgupta S, Bhattacharya S, Biswas A, Majumdar SS, Mukhopadhyay S, et al. (2010) NF-kappaB mediates lipid-induced fetuin-A expression in hepatocytes that impairs adipocyte function effecting insulin resistance. Biochem J 429: 451–462.
21. Gangneux C, Daveau M, Hiron M, Derambure C, Papaconstantinou J, et al. (2003) The inflammation-induced down-regulation of plasma Fetuin-A (alpha2HS-Glycoprotein) in liver results from the loss of interaction between long C/EBP isoforms at two neighbouring binding sites. Nucleic Acids Res 31: 5957–5970.
22. Yang Q, Graham TE, Mody N, Preitner F, Peroni OD, et al. (2005) Serum retinol binding protein 4 contributes to insulin resistance in obesity and type 2 diabetes. Nature 436: 356–362.
23. Vitkova M, Klimcakova E, Kovacikova M, Valle C, Moro C, et al. (2007) Plasma levels and adipose tissue messenger ribonucleic acid expression of retinol-binding protein 4 are reduced during calorie restriction in obese subjects but are not related to diet-induced changes in insulin sensitivity. J Clin Endocrinol Metab 92: 2330–2335.
24. Marshall WJ (2008) Nutritional assessment: its role in the provision of nutritional support. J Clin Pathol 61: 1083–1088.
25. van Lettow M, Fawzi WW, Semba RD (2003) Triple trouble: the role of malnutrition in tuberculosis and human immunodeficiency virus co-infection. Nutr Rev 61: 81–90.
26. Schultz DR, Arnold PI (1990) Properties of four acute phase proteins: C-reactive protein, serum amyloid A protein, alpha 1-acid glycoprotein, and fibrinogen. Semin Arthritis Rheum 20: 129–147.
27. Hang NT, Lien LT, Kobayashi N, Shimbo T, Sakurada S, et al. (2011) Analysis of factors lowering sensitivity of interferon-γ release assay for tuberculosis. PLoS One 6: e23806.
28. Sakurada S, Hang NT, Ishizuka N, Toyota E, Hung LD, et al. (2012) Inter-rater agreement in the assessment of abnormal chest X-ray findings for tuberculosis between two Asian countries. BMC Infect Dis 12: 31.
29. Santucci N, D'Attilio L, Kovalevski L, Bozza V, Besedovsky H, et al. (2011) A multifaceted analysis of immune-endocrine-metabolic alterations in patients with pulmonary tuberculosis. PLoS One 6: e26363.
30. Robinson K, Prins J, Venkatesh B (2011) Clinical review: adiponectin biology and its role in inflammation and critical illness. Crit Care 15: 221.
31. Langouche L, Vander Perre S, Frystyk J, Flyvbjerg A, Hansen TK, et al. (2009) Adiponectin, retinol-binding protein 4, and leptin in protracted critical illness of pulmonary origin. Crit Care 13: R112.
32. Walkey AJ, Rice TW, Konter J, Ouchi N, Shibata R, et al. (2010) Plasma adiponectin and mortality in critically ill subjects with acute respiratory failure. Crit Care Med 38: 2329–2334.
33. Moriconi N, Kraenzlin M, Müller B, Keller U, Nusbaumer CP, et al. (2006) Body composition and adiponectin serum concentrations in adult patients with cystic fibrosis. J Clin Endocrinol Metab 91: 1586–1590.
34. Sood A (2010) Obesity, adipokines, and lung disease. J Appl Physiol 108: 744–753.
35. Schwenk A, Hodgson L, Rayner CF, Griffin GE, Macallan DC (2003) Leptin and energy metabolism in pulmonary tuberculosis. Am J Clin Nutr 77: 392–398.
36. van Lettow M, van der Meer JW, West CE, van Crevel R, Semba RD (2005) Interleukin-6 and human immunodeficiency virus load, but not plasma leptin concentration, predict anorexia and wasting in adults with pulmonary tuberculosis in Malawi. J Clin Endocrinol Metab 90: 4771–4776.
37. van Crevel R, Karyadi E, Netea MG, Verhoef H, Nelwan RH, et al. (2002) Decreased plasma leptin concentrations in tuberculosis patients are associated with wasting and inflammation. J Clin Endocrinol Metab 87: 758–763.
38. Buyukoglan H, Gulmez I, Kelestimur F, Kart L, Oymak FS, et al. (2007) Leptin levels in various manifestations of pulmonary tuberculosis. Mediators Inflamm 2007: 64859.
39. Yuksel I, Sencan M, Dokmetas HS, Dokmetas I, Ataseven H, et al. (2003) The relation between serum leptin levels and body fat mass in patients with active lung tuberculosis. Endocr Res 29: 257–264.
40. Cakir B, Yonem A, Guler S, Odabasi E, Demirbas B, et al. (1999) Relation of leptin and tumour necrosis factor alpha to body weight changes in patients with pulmonary tuberculosis. Horm Res 52: 279–283.
41. Bornstein SR, Preas HL, Chrousos GP, Suffredini AF (1998) Circulating leptin levels during acute experimental endotoxemia anti-inflammatory therapy in humans. J Infect Dis 178: 887–890.
42. Kim JH, Lee CT, Yoon HI, Song J, Shin WG, et al. (2010) Relation of ghrelin, leptin and inflammatory markers to nutritional status in active pulmonary tuberculosis. Clin Nutr 29: 512–8.
43. Bruun JM, Pedersen SB, Kristensen K, Richelsen B (2002) Effects of pro-inflammatory cytokines and chemokines on leptin production in human adipose tissue in vitro. Mol Cell Endocrinol 190: 91–99.
44. Arnalich F, Lopez J, Codoceo R, Jim M, Madero R, et al. (1999) Relationship of plasma leptin to plasma cytokines and human survival in sepsis and septic shock. J Infect Dis 180: 908–911.
45. Gualillo O, Eiras S, Lago F, Diéguez C, Casanueva FF (2000) Elevated serum leptin concentrations induced by experimental acute inflammation. Life Sci 67: 2433–2441.
46. Wallace AM, Sattar N, Mcmillan DC (2000) The co-ordinated cytokine/hormone response to acute injury incorporates leptin. Cytokine 12: 1042–1045.
47. Satoh N, Naruse M, Usui T, Tagami T, Suganami T, et al. (2004) Leptin-to-adiponectin ratio as a potential atherogenic index in obese type 2 diabetic patients. Diabetes Care 27: 2488–2490.
48. Wieland CW, Florquin S, Chan ED, Leemans JC, Weijer S, et al. (2005) Pulmonary Mycobacterium tuberculosis infection in leptin-deficient ob/ob mice. Int Immunol 17: 1399–1408.
49. Jahnen-Dechent W, Schäfer C, Ketteler M, McKee MD (2008) Mineral chaperones: a role for fetuin-A and osteopontin in the inhibition and regression of pathologic calcification. J Mol Med (Berl) 86: 379–389.
50. Jersmann HP, Dransfield I, Hart SP (2003) Fetuin/alpha2-HS glycoprotein enhances phagocytosis of apoptotic cells and macropinocytosis by human macrophages. Clin Sci (Lond) 105: 273–278.
51. Koch A, Weiskirchen R, Sanson E, Zimmermann HW, Voigt S, et al. (2010) Circulating retinol binding protein 4 in critically ill patients before specific treatment: prognostic impact and correlation with organ function, metabolism and inflammation. Crit Care 14: R179.
52. Fuhrman MP, Charney P, Mueller CM (2004) Hepatic proteins and nutrition assessment. J Am Diet Assoc 104: 1258–1264.
53. Ingenbleek Y, Van Den Schrieck HG, De Nayer P, De Visscher M (1975) Albumin, transferrin and the thyroxine-binding prealbumin/retinol-binding protein (TBPA-RBP) complex in assessment of malnutrition. Clin Chim Acta 63: 61–67.
54. Gavrila A, Peng CK, Chan JL, Mietus JE, Goldberger AL, et al. (2003) Diurnal and ultradian dynamics of serum adiponectin in healthy men: comparison with leptin, circulating soluble leptin receptor, and cortisol patterns. J Clin Endocrinol Metab 88: 2838–2843.

Human Immunology 74 (2013) 395–401

Contents lists available at SciVerse ScienceDirect

journal homepage: www.elsevier.com/locate/humimm

Differential effects of a common splice site polymorphism on the generation of *OAS1* variants in human bronchial epithelial cells

Satoshi Noguchi [a,b], Emi Hamano [a,b], Ikumi Matsushita [a], Minako Hijikata [a], Hideyuki Ito [c], Takahide Nagase [b], Naoto Keicho [a,*]

[a] Department of Respiratory Diseases, Research Institute, National Center for Global Health and Medicine, Tokyo 162-8655, Japan
[b] Department of Respiratory Medicine, University of Tokyo Hospital, Tokyo 113-0033, Japan
[c] Department of Thoracic Surgery, National Center for Global Health and Medicine, Tokyo 162-8655, Japan

ARTICLE INFO

Article history:
Received 5 June 2012
Accepted 27 November 2012
Available online 5 December 2012

ABSTRACT

The 2′,5′-oligoadenylate synthetase 1 (*OAS1*) is one of the major interferon-inducible proteins and a critical component of the host defense system against viral infection. A single nucleotide polymorphism (SNP), rs10774671, presumably responsible for alternate splicing of this gene, has frequently been associated with a variety of viral diseases, including emerging respiratory infections. We investigated the SNP-dependent expression of *OAS1* variants in primary cultured human bronchial epithelial cells. Total RNA was subjected to real-time RT-PCR with specific primer sets designed to amplify each transcript variant. We found that the p46 transcript was mainly expressed in cells with the GG genotype, whereas the p42 transcript was highly expressed, and the p44a (alternate exon in intron 5), p48, and p52 transcripts were expressed to a lesser extent, in cells with the AA genotype. Immunoblot analysis revealed that the p46 isoform and a smaller amount of the p42 isoform were present in cells with the GG genotype, whereas only the p42 isoform was clearly observed in cells with the AA genotype. Cellular DNA fragmentation induced by neutrophil elastase was more preferentially found in cells with the AA genotype. Thus, our findings provide insights into the potential role of *OAS1* polymorphisms in respiratory infection.

1. Introduction

Innate immune responses are the first line of defenses against viruses. When viral infection is detected by pattern recognition receptors, infected cells produce type I (α and β) and type III (λ) interferons (IFNs) [1]. Binding of IFNs to their specific receptors leads to the induction of more than 300 IFN-stimulated genes, including *OAS1*, which encodes the enzyme 2′,5′-oligoadenylate synthetase 1 (*OAS1*) [2]. Typically, OAS1 is activated by the binding of double-stranded RNA and catalyzes the oligomerization of ATP into 2′,5′-linked oligoadenylates (2-5A) [3,4]. These 2-5A, in turn, bind to latent ribonuclease L (RNase L), which then dimerizes into an active form. The activated RNase L degrades viral and cellular single-stranded RNA [5].

Eight isoforms of *OAS1* with different carboxyl (C)-terminal amino acid sequences have been registered in the public database. Among them, the p42, p46, and p48 isoforms were found earlier and their functions have been studied well [6]. The C-terminal tail of the p48 isoform has a unique Bcl-2 homology-3 (BH3) domain, which interacts with anti-apoptotic proteins of the Bcl-2 family [7]. Therefore, the p48 isoform may have dual functions, potentiating apoptosis through the BH3 domain as well as activating RNase L via the classical anti-viral pathway [8,9].

Bonnevie–Nielsen et al. have demonstrated that an A/G single nucleotide polymorphism (SNP) at the splice acceptor site of exon 6 (rs10774671) contributes to generation of these three isoforms through alternative splicing [10]. According to their study using human lymphocytes, the G allele generates the p46 transcript, while the A allele abrogates the production of the p46 transcript and drives splicing to occur further downstream, leading to generation of the p48 and p52 transcripts.

To date, polymorphisms of *OAS1* and other immune-related genes have been reported to affect susceptibility to a variety of viral diseases [11]. In mice, a single missense mutation of the 2′,5′-oligoadenylate synthetase 1B (*Oas1b*) gene, a murine ortholog of *OAS1*, determines resistance to flaviviruses, including West Nile virus (WNV) [12,13]. In humans, the A allele of SNP rs10774671 in *OAS1* was associated with susceptibility to infection with WNV [14]. An *OAS1* SNP (rs2660) in strong linkage disequilibrium (LD)

Abbreviations: LD, linkage disequilibrium; HBE, human bronchial epithelial cells; SARS, severe acute respiratory syndrome; NE, neutrophil elastase.

* Corresponding author. Address: Department of Respiratory Diseases, Research Institute, National Center for Global Health and Medicine, 1-21-1 Toyama, Shinjuku-ku, Tokyo 162-8655, Japan. Fax: +81 3 3202 7364.
E-mail address: nkeicho-tky@umin.ac.jp (N. Keicho).

0198-8859/$36.00 - see front matter © 2012 American Society for Histocompatibility and Immunogenetics. Published by Elsevier Inc. All rights reserved.
http://dx.doi.org/10.1016/j.humimm.2012.11.011

with rs10774671 [10] was also associated with the outcome of hepatitis C virus (HCV) infection [15]. However, the allele associated with susceptibility to infection varied among studies, and the production of different *OAS1* isoforms have not yet been fully investigated [16]. Considering that the interactions between virus and host are complex and cell-type-specific, *OAS1* expression patterns should be characterized in a particular cell type infected by a virus of interest. In particular, host genetic factors affecting the airway defense mechanism against emerging respiratory viral infections, such as severe acute respiratory syndrome (SARS) and avian influenza, which pose potential global threats, should be studied intensively in preparation for future outbreaks.

We previously reported association of *OAS1* polymorphisms with susceptibility to infection by the SARS coronavirus in Vietnamese population [17]. In the present study, we investigated the splice site SNP (rs10774671)-dependent expression of transcript variants and production of functional isoforms of *OAS1* in primary cultured human bronchial epithelial (HBE) cells, a site for replication of many respiratory viruses.

2. Materials and methods

2.1. Cell culture

The ethical committee of National Center for Global Health and Medicine (formerly International Medical Center of Japan) approved the study protocol. Primary cultured HBE cells were obtained from the cancer-free bronchi of surgically resected lungs, after obtaining written informed consent from the individuals concerned, all of whom were Japanese.

We isolated and cultured HBE cells from the resected lung tissue as previously described [18], and cells of passages 3–5 were used in this study. Briefly, HBE cells were seeded at a density of 5×10^5/well onto collagen-coated 6-well Transwell plates (Corning, Corning, NY, USA) and cultured in bronchial epithelial growth medium (BEGM; Biowhittaker, Walkersville, MD, USA) for 24 h. Thereafter, cells were stimulated with 1000 IU/ml IFN-β (Biosource International, Camarillo, CA, USA) for 18 h and then harvested.

2.2. DNA isolation and genotyping of the SNP at the splice acceptor site

Genomic DNA was extracted from HBE cells using the QIAamp DNA Mini Kit (QIAGEN, Hamburg, Germany). The SNP rs10774671 was genotyped utilizing PCR and restriction fragment length polymorphism (RFLP) methods. Genomic DNA was amplified using AmpliTaq Gold DNA polymerase (Applied Biosystems, Foster City, CA, USA) with the primers listed in Supplementary Table 1. The cycling conditions involved 45 cycles at 95 °C for 15 s, 55 °C for 15 s, and 72 °C for 30 s. The PCR products (532 bp) were digested with *Alu* I (New England Biolabs, Ipswich, MA, USA) at 37 °C for 2 h, and were then electrophoresed on 3% agarose gels including ethidium bromide. Genotypes were determined by the size of the digested PCR products observed upon visualization of the gels (306, 181, 33, and 12 bp for the G allele and 255, 181, 51, 33, and 12 bp for the A allele).

2.3. Real-time reverse transcription (RT)-PCR

We selected HBE cells with AA ($n = 6$), AG ($n = 3$), and GG ($n = 2$) genotypes of rs10774671; these cells were stimulated with IFN-β. Total RNA was extracted using an RNeasy Mini Kit (QIAGEN). One microgram of the total RNA was subjected to RT with random nonamers using SuperScript III Reverse Transcriptase (Invitrogen, Carlsbad, CA, USA), as recommended by the manufacturer. Expression of *OAS1* mRNA was analyzed by real-time RT-PCR using Power SYBR Green PCR Master Mix (Applied Biosystems) and CFX96 (Bio-Rad, Hercules, CA, USA) according to the manufacturer's instructions.

Previous reports indicated that *OAS1* can give rise to as many as eight alternatively spliced transcripts [16,19,20]. A primer set common to all transcript variants was used to amplify all *OAS1* transcripts, and transcript-specific primer sets were used to amplify each transcript. Primers and annealing/extension temperatures are listed in Table 1. The cycling conditions were as follows: initial activation of the Taq DNA Polymerase for 10 min at 95 °C, followed by 40 cycles of 15 s denaturation at 95 °C, and annealing and extension for 1 min at the appropriate temperature. Specific amplification of the target was confirmed by a single peak in the dissociation curve and by visualization of the expected size of RT-PCR products on an agarose gel.

To compare the mRNA copy numbers among transcript variants, the absolute quantification method was used [21]. Isoform-specific RT-PCR products containing the target sequences, amplified with primers in Supplementary Table 1, were purified using the Wizard PCR Preps DNA Purification System (Promega, Fitchburg, WI, USA). Their copy numbers were calculated from the concentration of DNA determined by measuring absorbance at 260 nm. The standard curve was generated with serial 5-fold dilutions of each of the RT-PCR products. The linear dependence of the threshold cycles was confirmed from the concentration of the templates. We used the β-actin gene (primers in Supplementary Table 1) to normalize

Table 1
OAS1 isoforms and real-time RT-PCR conditions.

Serial number	Isoform	GenBank accession no.	Expected protein sizes (kDa)	Real-time RT-PCR primers	Nucleotide sequences (5′ → 3′)	Annealing and extension temperature (°C)
1	p42	NM_002534.2	41.7	Forward	ACCTGAGAAGGCAGCTCACGAAAC	60
				Reverse	CAGGGAGGAAGCAGGAGGTCTCAC	
2	p46	NM_016816.2	46.0	Forward	ACCTGAGAAGGCAGCTCACGAAAC	68
				Reverse	ATCGTCTGTACTGTTGCTTTCAGCC	
3	p23	AK301498.1	22.8	N/T*		
4	p35	AK300346	35.4	Forward	CTCATCCGCCTAGTCAAGCAC	60
				Reverse	CCAAGGCACTGTACCTGTATCC	
5	p44a	CF272298	44.1	Forward	ACCTGAGAAGGCAGCTCACGAAAC	66
				Reverse	CATTTCCACCACTTGTTAGCTGATGTC	
6	p52	AY730627.1	52.1	Forward	ACCTGAGAAGGCAGCTCACGAAAC	68
				Reverse	ATCGTCTGTACTGTTGCTTTCAGCA	
7	p48	NM_001032409.1	47.4	Forward	ACCTGAGAAGGCAGCTCACGAAAC	68
				Reverse	GCTGCCTGGAGTGTGCTGGGTCAG	
8	p44b	AJ629455.1	43.9	Forward	ACCTGAGAAGGCAGCTCACGAAAC	60
				Reverse	TAGTTCCTTCTGCCAACCAGTGTG	

* Not tested.

OAS1 expression. Fold-changes of total *OAS1* expression with IFN-β and relative mRNA amounts of each transcript with respect to the amount of mRNA for the p42 transcript in AA cells without stimulation of IFN-β were calculated. Data are expressed as the mean ± standard error of the mean (SEM).

2.4. Immunoblot analysis

HBE cells with AA ($n = 8$), AG ($n = 3$), and GG ($n = 2$) genotypes of rs10774671 were stimulated with IFN-β and harvested with lysis buffer Complete Lysis-M, EDTA-free buffer (Roche Applied Science, Penzberg, Germany). The total protein concentration in each sample was measured using the BioRad Protein Assay (BioRad). Equal amounts of total protein from each lysate (20 μg/lane) was resuspended in SDS buffer (125 mM Tris–HCl, pH 6.8, 10% glycerol, 2% SDS, 1.55% dithiothreitol, and 0.1% bromophenol blue), boiled for 5 min, and analyzed on a 10% SDS–PAGE gel (e-PAGEL; ATTO, Tokyo, Japan). Resolved proteins were transferred to a polyvinylidene difluoride membrane (Millipore, Billerica, MA, USA). After blocking the membrane in Tris-buffered saline with 0.1% Tween 20 and 2% blocking reagent at 4 °C overnight, blots were hybridized for 1 h at room temperature with primary antibody against the protein fragment (amino acids 80–221) common to all OAS1 isoforms (Sigma–Aldrich, St. Louis, MO, USA; product number, HPA003657), at a dilution of 1:1000. After hybridization with horseradish peroxidase-conjugated secondary antibody, the immunocomplexes were visualized using an ECL Western blotting detection system (GE Healthcare, Little Chalfont, United Kingdom). The intensity of each band was semi-quantitatively determined using a densitometer with the Quantity One 1-D software (BioRad). The same blot was reprobed with anti-β-tubulin monoclonal antibody (Thermo Fisher Scientific, Waltham, MA, USA) as a loading control.

2.5. Rapid amplification of cDNA ends (5′-RACE and 3′-RACE)

RNA ligase-mediated rapid amplification of cDNA ends (RLM-RACE) was carried out using total RNA from IFN-β-stimulated HBE cells with AA or GG genotypes of rs10774671, using the First-Choice RLM-RACE Kit (Ambion, Austin, TX, USA) according to the manufacturer's instructions. Gene-specific primers are listed in Supplementary Table 1. PCR products were purified and sequenced with the BigDye Terminator v3.1 Cycle Sequencing Kit (Applied Biosystems) using a 3100 Genetic Analyzer (Applied Biosystems). PCR products from 3′-RACE were electrophoresed on 2% agarose gels containing ethidium bromide.

2.6. SNP screening of OAS1 gene

Information about SNP genotypes of *OAS1* in the Japanese population from Tokyo (JPT) was obtained from HapMap data sets [22], and was analyzed using Haploview (v. 4.2) [23]. LD blocks were determined using the confidence interval method [24]. Tag SNPs were selected and genotyped from the DNA of study participants.

In addition, we screened genetic polymorphisms from the promoter region [6] to exon 6 of *OAS1*, using 4 DNA samples with genotypes representing the tag SNP. The entire region was amplified using three overlapping PCR products. Primers are listed in Supplementary Table 1. Amplified products were purified and sequenced using appropriate inner primers as described above.

2.7. DNA fragmentation ELISA

HBE cells with AA ($n = 5$) and GG ($n = 3$) genotypes of rs10774671 were stimulated with or without IFN-β (1000 IU/ml) for 12 h, were further treated with 5×10^{-8} M neutrophil elastase (NE; Elastin Products Company, Owensville, MO, USA) for 6 h. Then, cells were pelleted and lysed, and apoptosis assessed using a cell death detection ELISA system (Cell Death Detection ELISA PLUS; Roche Applied Science). Enrichment for mono- and oligonucleosomes released into the cytoplasmic fractions of cell lysates was detected by biotinylated antihistone- and peroxidase-coupled anti-DNA antibodies. The relative absorbance ratio (absorbance of sample cells/absorbance of control cells) was calculated in triplicate, and used as a parameter of DNA fragmentation.

2.8. Statistical analysis

All data were expressed as mean ± SEM. To assess the effect of the number of A (or G) alleles on expression levels of transcript variants, a linear regression model was applied (JMP, version 9.0.0; SAS Institute Inc., Cary, NC, USA). Relative absorbance ratio from the apoptosis assay was analyzed by the unpaired Student's *t*-test. Differences were considered to be statistically significant when $p < 0.05$.

3. Results

3.1. Difference in OAS1 expression between AA, AG, and GG genotypes

According to previous reports, *OAS1* gives rise to eight alternatively spliced transcripts [16,19,20], and the corresponding gene products with various molecular weights are shown in Fig. 1 and Table 1. Supplementary Fig. 1 shows the results of RT-PCR with primer sets designed to specifically amplify each transcript variant. We did not detect the p23 transcript in HBE cells with any of the three genotypes.

We next analyzed the total and transcript-specific expression of *OAS1* in the presence or absence of IFN-β stimulation by real-time RT-PCR (Fig. 2). When HBE cells were stimulated with IFN-β, total *OAS1* expression was increased up to 20-fold, irrespective of genotype ($p = 0.432$). Of the splicing variants, p42 was the main transcript expressed in HBE cells with the AA genotype, whereas p46 transcripts were predominant in those with the GG genotype. Expression of the p46 transcript was significantly higher in proportion to the number of G alleles carried by HBE cells, under both unstimulated and stimulated conditions ($p < 0.001$, $p < 0.001$). By contrast, expression of the p42, p44a (alternate exon in intron 5), p52, and p48 transcripts was all higher in proportion to the number of A alleles present in the cells, under both unstimulated and stimulated conditions (p42: $p < 0.001$, $p < 0.001$; p44a: $p = 0.014$,

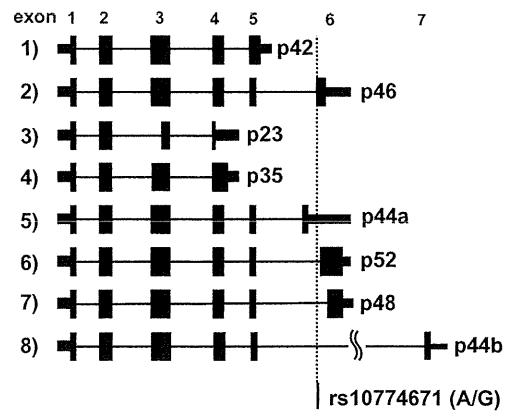

Fig. 1. Schematic representation of *OAS1* transcript variants. Alternatively spliced exons, the predicted protein size, and the position of the SNP at the splice acceptor site (rs10774671) are shown. The number in parenthesis indicates each transcript, corresponding to that in Table 1. Coding regions are indicated by wide rectangles, noncoding regions by narrow rectangles, and introns by lines. We designated the isoform with an alternate exon in intron 5 as p44a, and that with exon7 as p44b.

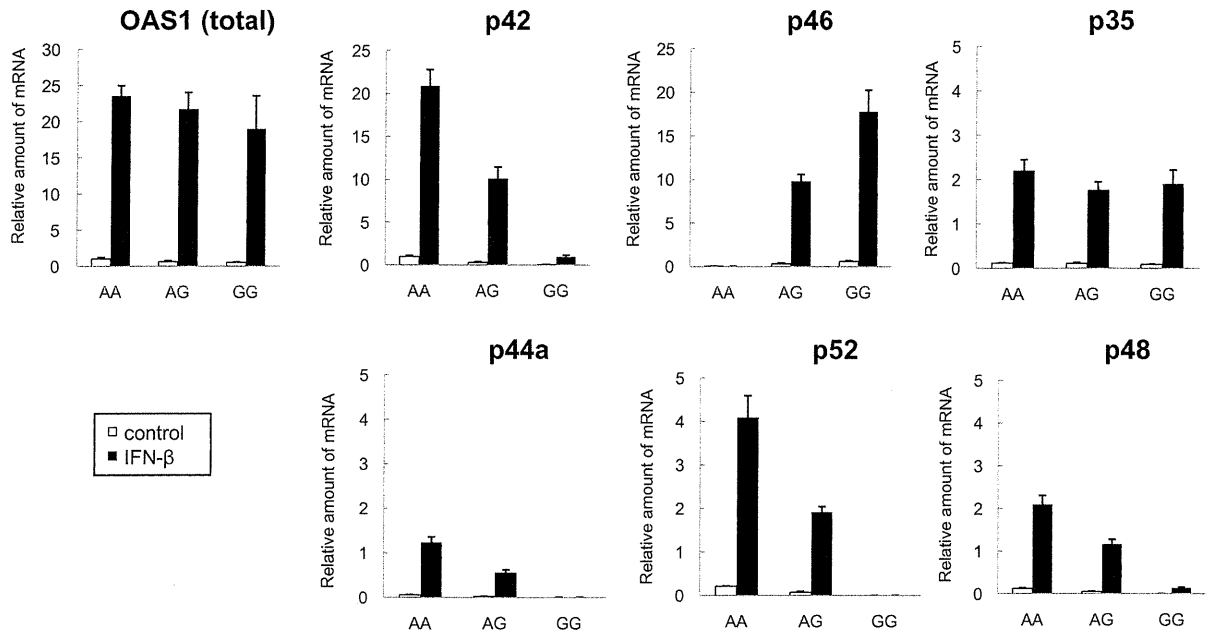

Fig. 2. Difference in the amount of transcript variants among genotypes in HBE cells. The expression of total *OAS1* and that of each individual transcript variant in HBE cells with the AA ($n = 6$), AG ($n = 3$), or GG ($n = 2$) genotypes of rs10774671 was obtained by real-time RT-PCR. Fold-inductions of total *OAS1* expression by IFN-β, and the relative mRNA amounts of each transcript over that of the p42 transcript in AA cells without stimulation of IFN-β are shown as mean ± SEM.

$p < 0.001$; p52: $p < 0.001$, $p = 0.013$; p48: $p < 0.001$, $p = 0.001$). Expression of the p35 transcript was not associated with either allele under both conditions ($p = 0.245$, $p = 0.495$). We did not quantify the p44b transcript containing exon 7 because the threshold cycle number was high and non-specific PCR amplification was observed.

Immunoblot analysis demonstrated expression of the p46 isoform and a low level of p42 in HBE cells with the GG and AG genotypes; another faint band slightly smaller than p46 was also detected. In cells with the AA genotype, only the p42 isoform was distinctly observed (Fig. 3). To compare the protein levels with the corresponding mRNA expression levels, the band intensity corresponding to each protein isoform was semi-quantified. While the p46 transcript was expressed approximately 20-fold more than the p42 transcript at the mRNA level in the GG cells stimulated with IFN-β, the p46 isoform was expressed only 2.2-fold more than the p42 isoform at the protein level.

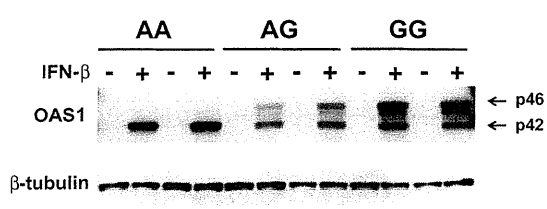

Fig. 3. Difference in the expression of *OAS1* isoforms among genotypes. Western blotting was performed using antibody against the epitope common to all isoforms of OAS1. HBE cells with AA ($n = 8$), AG ($n = 3$), and GG ($n = 2$) genotypes of rs10774671 were analyzed, and the isoform expression pattern was the same in each genotype. Two representative results in each genotype are shown. As a loading control, the same blot was reprobed with anti-β-tubulin monoclonal antibody (bottom part).

3.2. Identification of the transcription start site of OAS1 in cells with the AA and GG genotypes

Using 5′-RACE, we found that the transcription start site of *OAS1* was 81 bp upstream of the translation start site in IFN-β-stimulated HBE cells with the AA and GG genotypes, indicating that the transcription start site did not differ between the genotypes. Using the 3′-RACE method, we showed that the p42, p48, and p52 transcripts were present in HBE cells with the AA genotype, while only the p42 and p46 transcripts were identified in those with the GG genotype (Supplementary Fig. 2). No other novel transcripts were amplified.

3.3. Search for other genetic polymorphisms and LD structures of OAS1

To search for other variants which may influence gene expression, we further analyzed nucleotide sequences throughout the region from the promoter to exon 6 and investigated the LD structure of *OAS1*. We selected rs3741981 (non-synonymous; exon 3), rs4766662 (intron 1), rs2240190 (intron 1), and rs10774671 as tag SNPs for genotyping. The exon 3 SNP was in complete LD with rs10774671 ($D' = 1$, $r^2 = 0.38$). The minor allele frequency of rs4766662 was less than 5%, while rs2240190 was not in LD with rs10774671 ($D' = 0.4$, $r^2 = 0.13$).

The SNP genotypes indicated that only SNPs in the region between intron 3 and exon 6 were in strong LD ($r^2 > 0.8$) with rs10774671. The LD block was bordered by exon 3, and we did not identify any SNP in strong LD with rs10774671 in the region extending from the promoter to intron 2. The LD pattern derived in our study was consistent with that obtained from the HapMap data (Supplementary Fig. 3).

3.4. DNA fragmentation assay

Since a previous report [7] suggested that the p48 isoform potentiates apoptosis through the BH3 domain in its specific C-ter-

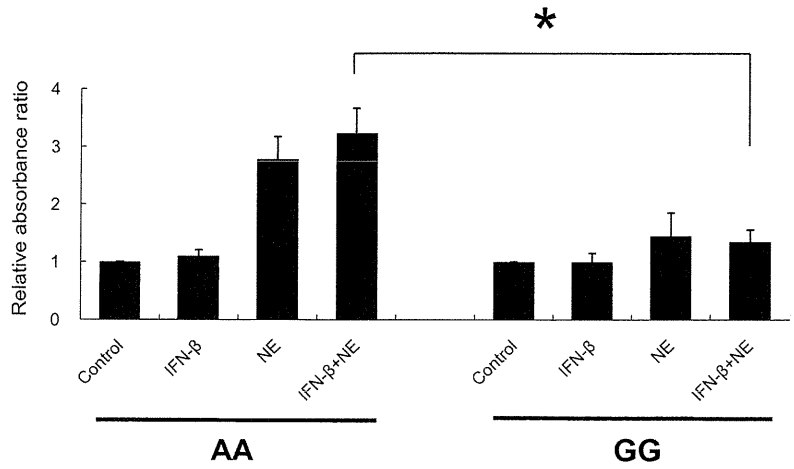

Fig. 4. Difference in DNA fragmentation between AA and GG genotypes. HBE cells with AA ($n = 5$) or GG ($n = 3$) genotypes were stimulated with IFN-β (1000 IU/ml) for 12 h and/or with NE (5×10^{-8} M) for 6 h. With an apoptosis determination kit, relative absorbance ratios (absorbance of sample cells/absorbance of control cells) were obtained and shown as mean ± SEM. Experiments were performed in triplicate. Statistically significant: $^{*}p < 0.05$.

minal, HBE cells were pretreated with IFN-β and further incubated with NE, an apoptosis-inducing agent. Although NE itself did not affect *OAS1* expression, as assessed by immunoblot analysis (data not shown), treatment with NE and IFN-β caused a larger amount of DNA fragmentation in cells with the AA genotype than in those with the GG genotype ($p = 0.021$). The genotype-dependent difference caused by NE in the absence of IFN-β did not reach significant levels ($p = 0.068$, Fig. 4).

4. Discussion

In this study, we investigated the differential effects of a splice site SNP on expression of transcript variants and production of functional isoforms of *OAS1* in primary cultured bronchial epithelial cells isolated from human lung, a major site of replication for respiratory viruses. We clearly demonstrated the G allele-dependent expression of the p46 isoform and the A allele-dependent expression of the p42, p44a, p48, and p52 transcripts. Expression of the p35 transcript did not differ among genotypes.

The G allele-dependent expression of p46 and the A allele-dependent expression of p48 and p52 in HBE cells were consistent with the pioneering report of Bonnevie-Nielsen et al. using human lymphocytes [10]. Prior to their report, such a common splice site SNP had not been identified, and the expression patterns of *OAS1* transcript variants had been assumed to be cell-type specific [25,26].

Furthermore, recent RNA sequencing studies using lymphoblast cell lines revealed that not only p48 and p52 transcripts but also p42 and p44a transcripts are expressed when the A allele is present [19,27]. We confirmed these observations in primary cultured HBE cells. However, the read-through transcript of intron 4 was amplified with the full exon 3 (p35 transcript). The short exon 3 using the alternative splice acceptor site within the exon 3 (p23 transcript) reported in lymphoblast cell lines [19] was not observed in our study.

The total amount of *OAS1* mRNA expression appeared to be slightly lower in proportion to the number of G alleles present, but this tendency was not statistically significant. In a previous study on HIV patients, significantly lower expression of *OAS1* was observed in peripheral blood mononuclear cells carrying the G allele of rs3177979, which is in LD with the G allele of rs10774671 [28]. Conversely, there was a 1.9-fold higher expression in lymphoblastoid cell lines with the GG genotype of rs10774671 than in those with the AG genotype [19]. This discrepancy may have been caused by differences in ethnicity or cell type.

Since the transcription start site was the same for transcripts arising from the A allele and the G allele, and because there was no SNP in the 5′-region of the gene that was in strong LD with rs10774671 according to both our SNP screening and analyses of HapMap data, the transcriptional activity resulting in each transcript variant is presumably similar. Thus, their expression levels would be expected to be determined by the efficiency of splicing and mRNA stability.

Immunoblot analysis revealed that the p46 isoform, and a lower level of p42, were detected in cells with the GG genotype. Interestingly, the amount of p42 isoform was about half that of the p46 isoform in the GG cells at the protein level, although mRNA expression of the p42 transcript was markedly lower than that of the p46 transcript in those cells. Laronde et al. reported that the p42 transcript accounted for 5% of the total *OAS1* transcripts in a lymphoblast cell line with a GG genotype, as determined by RNA sequencing [19]; this was in accord with the results obtained from our absolute quantification method. The translational efficiency may differ between p42 and p46 transcripts because they have distinct 3′-UTR sequences that may differentially bind to RNA-binding proteins [29] or to micro RNAs [30]. In Daudi lymphoid cells with a GG genotype [10], only the p46 isoform was detected [26]. Therefore, expression of the p42 isoform in cells bearing a GG genotype may be specific to the cell type, presumably through tissue-specific regulation of alternative splicing [31].

Another band slightly smaller than p46 was observed in the G allele-carrying cells. A similar band was also visible in Daudi cells with the GG genotype [26]. Thus far, the isoform corresponding to this size has not been identified, and we did not find any novel transcript by 3′-RACE. The band may indicate some degradation of the p46 isoform, although there is no evidence that the C-terminal tail contains a cleavage site.

We predominantly detected the p42 isoform, but not p46 in the cells with the AA genotype, under the same immunoblotting condition. The other isoforms (p35, p44a, p48, and p52), of which the transcripts could be amplified in the AA cells by real-time RT-PCR, were not detected either, possibly because of their low expression levels.

Only a few studies have been conducted on the differences in the function of different isoforms. Bonnevie-Nielsen et al. reported

that the total enzyme activity of *OAS1* in unstimulated lymphocytes was highest in individuals with the GG genotype, intermediate in those with the AG genotype, and lowest in those with the AA genotype. They raised the possibility that the p46 isoform, arising from the G allele, has higher enzymatic activity than the p48 and p52 isoforms arising from the A allele. This suggests that individuals carrying the A allele are more susceptible to some viruses; consequently, Lim et al. demonstrated that the A allele was associated with susceptibility to WNV infection and that WNV replicated to higher levels in lymphoid tissues from donors carrying the A allele [14]. Lin et al. reported that p42 and p46, but not the other *OAS1* isoforms (p44b, p48, and p52), blocked dengue viral replication via an RNase L-dependent mechanism [16]. Since HBE cells produce a considerable amount of the p42 isoform in the presence of the AA genotype, functional roles of the A allele are worth reconsidering in respiratory virus infection.

In our study, NE-induced cellular DNA fragmentation was preferentially found in HBE cells with the AA genotype when stimulated with IFN-β. NE is a major apoptotic inducer in inflamed airway epithelium, and Suzuki et al. showed molecular mechanisms of leukocyte elastase-induced apoptosis in HBE cells [32]. We also found that NE increased the level of annexin-V staining in an immortalized HBE cell line, BEAS-2B (unpublished observation). However, we could not further investigate other key features of apoptosis than DNA fragmentation in the present study, because the number of experiments using primary cultured cells had limitations. Since the p48 isoform arising from the A allele was previously shown to have proapoptotic activity independent of RNase L activation [7], it is conceivable that the increased DNA fragmentation in HBE cells with the AA genotype is attributed to this unique activity of the p48 isoform that is presumably absent in the cells with the GG genotype. RNase L activation may not be involved in the difference observed in the present study because OAS enzymatic activity is detectable in the presence of exogenous dsRNA [4]. However, it remains elusive whether genotypic differences in DNA fragmentation was derived from the p48 isoform, because its protein expression was not detected by the sensitivity of Western blotting. Alternatively, the predominant p42 isoform in cells bearing the AA genotype may be related to DNA fragmentation through an unknown mechanism. It is generally known that apoptosis can contribute to protection against viral infection by killing virus-infected cells, but it may also serve as a mechanism for virus-induced tissue injury and progression of disease [33]. We have postulated that HBE cells carrying the A allele are more likely to inhibit spreading of the virus infection through promotion of apoptosis of virus-infected cells; thus, the A allele is associated with resistance to SARS infection [17]. Our findings indicate a requirement for further understanding of allele-specific functions other than classical enzymatic activity of OAS isoforms.

The G allele of rs10774671 is possibly an ancestral type because it had been identified in hominoid primates (*Pan troglodytes*), Old World monkeys (*Macaca mulatta*), and New World monkeys (*Callithrix jacchus*), according to the sequence data from public databases. Additionally, a recent study reported that the region carrying the splice site variant was neutrally evolving [20]. It is intriguing to speculate that the G to A substitution of rs10774671 generated isoforms with low enzymatic activity and high apoptosis-inducing activity, resulting in maintaining the balance between resistance and susceptibility to viral infection.

In conclusion, we have characterized the rs10774671 SNP-dependent expression profile of *OAS1* transcript variants and isoforms with possibly different functions in primary cultured HBE cells. Our findings may lead to an improved understanding of the association of *OAS1* gene with susceptibility to infection with respiratory viruses.

Acknowledgments

We thank Keiko Wakabayashi and Fumi Toshioka for their technical assistance in the study. This work was partly supported by a grant of National Center for Global Health and Medicine.

Appendix A. Supplementary data

Supplementary data associated with this article can be found, in the online version, at http://dx.doi.org/10.1016/j.humimm.2012.11.011.

References

[1] Randall RE, Goodbourn S. Interferons and viruses: an interplay between induction, signalling, antiviral responses and virus countermeasures. J Gen Virol 2008;89:1–47.
[2] Sadler AJ, Williams BR. Interferon-inducible antiviral effectors. Nat Rev Immunol 2008;8:559–68.
[3] Hovanessian AG, Justesen J. The human 2'-5'oligoadenylate synthetase family: unique interferon-inducible enzymes catalyzing 2'-5' instead of 3'-5' phosphodiester bond formation. Biochimie 2007;89:779–88.
[4] Kristiansen H, Gad HH, Eskildsen-Larsen S, Despres P, Hartmann R. The oligoadenylate synthetase family: an ancient protein family with multiple antiviral activities. J Interferon Cytokine Res 2011;31:41–7.
[5] Chakrabarti A, Jha BK, Silverman RH. New insights into the role of RNase L in innate immunity. J Interferon Cytokine Res 2011;31:49–57.
[6] Justesen J, Hartmann R, Kjeldgaard NO. Gene structure and function of the 2'-5'-oligoadenylate synthetase family. Cell Mol Life Sci 2000;57:1593–612.
[7] Ghosh A, Sarkar SN, Rowe TM, Sen GC. A specific isozyme of 2'-5' oligoadenylate synthetase is a dual function proapoptotic protein of the Bcl-2 family. J Biol Chem 2001;276:25447–55.
[8] Domingo-Gil E, Esteban M. Role of mitochondria in apoptosis induced by the 2–5A system and mechanisms involved. Apoptosis 2006;11:725–38.
[9] Castelli JC, Hassel BA, Maran A, Paranjape J, Hewitt JA, Li XL, et al. The role of 2'-5' oligoadenylate-activated ribonuclease L in apoptosis. Cell Death Differ 1998;5:313–20.
[10] Bonnevie-Nielsen V, Field LL, Lu S, Zheng DJ, Li M, Martensen PM, et al. Variation in antiviral 2',5'-oligoadenylate synthetase (2'5'AS) enzyme activity is controlled by a single-nucleotide polymorphism at a splice-acceptor site in the OAS1 gene. Am J Hum Genet 2005;76:623–33.
[11] Burgner D, Jamieson SE, Blackwell JM. Genetic susceptibility to infectious diseases: big is beautiful, but will bigger be even better? Lancet Infect Dis 2006;6:653–63.
[12] Mashimo T. A nonsense mutation in the gene encoding 2'-5'-oligoadenylate synthetase/L1 isoform is associated with West Nile virus susceptibility in laboratory mice. Proc Natl Acad Sci USA 2002;99:11311–6.
[13] Perelygin AA. Positional cloning of the murine flavivirus resistance gene. Proc Natl Acad Sci USA 2002;99:9322–7.
[14] Lim JK, Lisco A, McDermott DH, Huynh L, Ward JM, Johnson B, et al. Genetic variation in OAS1 is a risk factor for initial infection with West Nile virus in man. PLoS Pathog 2009;5:e1000321.
[15] Knapp S, Yee LJ, Frodsham AJ, Hennig BJ, Hellier S, Zhang L, et al. Polymorphisms in interferon-induced genes and the outcome of hepatitis C virus infection: roles of MxA, OAS-1 and PKR. Genes Immun 2003;4:411–9.
[16] Lin RJ, Yu HP, Chang BL, Tang WC, Liao CL, Lin YL. Distinct antiviral roles for human 2',5'-oligoadenylate synthetase family members against dengue virus infection. J Immunol 2009;183:8035–43.
[17] Hamano E, Hijikata M, Itoyama S, Quy T, Phi NC, Long HT, et al. Polymorphisms of interferon-inducible genes OAS-1 and MxA associated with SARS in the Vietnamese population. Biochem Biophys Res Commun 2005;329:1234–9.
[18] Gray TE, Guzman K, Davis CW, Abdullah LH, Nettesheim P. Mucociliary differentiation of serially passaged normal human tracheobronchial epithelial cells. Am J Respir Cell Mol Biol 1996;14:104–12.
[19] Lalonde E, Ha KC, Wang Z, Bemmo A, Kleinman CL, Kwan T, et al. RNA sequencing reveals the role of splicing polymorphisms in regulating human gene expression. Genome Res 2011;21:545–54.
[20] Cagliani R, Fumagalli M, Guerini FR, Riva S, Galimberti D, Comi GP, et al. Identification of a new susceptibility variant for multiple sclerosis in OAS1 by population genetics analysis. Hum Genet 2012;131:87–97.
[21] Leong DT, Gupta A, Bai HF, Wan G, Yoong LF, Too HP, et al. Absolute quantification of gene expression in biomaterials research using real-time PCR. Biomaterials 2007;28:203–10.
[22] A haplotype map of the human genome. Nature 2005;437:1299–320.
[23] Barrett JC, Fry B, Maller J, Daly MJ. Haploview: analysis and visualization of LD and haplotype maps. Bioinformatics 2005;21:263–5.
[24] Gabriel SB, Schaffner SF, Nguyen H, Moore JM, Roy J, Blumenstiel B, et al. The structure of haplotype blocks in the human genome. Science 2002;296:2225–9.

[25] Benech P, Merlin G, Revel M, Chebath J. 3' end structure of the human (2'-5') oligo A synthetase gene: prediction of two distinct proteins with cell type-specific expression. Nucleic Acids Res 1985;13:1267–81.
[26] Chebath J, Benech P, Hovanessian A, Galabru J, Revel M. Four different forms of interferon-induced 2',5'-oligo(A) synthetase identified by immunoblotting in human cells. J Biol Chem 1987;262:3852–7.
[27] Pickrell JK, Marioni JC, Pai AA, Degner JF, Engelhardt BE, Nkadori E, et al. Understanding mechanisms underlying human gene expression variation with RNA sequencing. Nature 2010;464:768–72.
[28] Rotger M, Dang KK, Fellay J, Heinzen EL, Feng S, Descombes P, et al. Genome-wide mRNA expression correlates of viral control in CD4+ T-cells from HIV-1-infected individuals. PLoS Pathog 2010;6:e1000781.
[29] Glisovic T, Bachorik JL, Yong J, Dreyfuss G. RNA-binding proteins and post-transcriptional gene regulation. FEBS Lett 2008;582:1977–86.
[30] Fabian MR, Sonenberg N, Filipowicz W. Regulation of mRNA translation and stability by microRNAs. Annu Rev Biochem 2010;79:351–79.
[31] Heinzen EL, Ge D, Cronin KD, Maia JM, Shianna KV, Gabriel WN, et al. Tissue-specific genetic control of splicing: implications for the study of complex traits. PLoS Biol 2008;6:e1.
[32] Suzuki T, Yamashita C, Zemans RL, Briones N, Van Linden A, Downey GP. Leukocyte elastase induces lung epithelial apoptosis via a PAR-1-, NF-kappaB-, and p53-dependent pathway. Am J Respir Cell Mol Biol 2009;41:742–55.
[33] Kaminskyy V, Zhivotovsky B. To kill or be killed: how viruses interact with the cell death machinery. J Intern Med 2010;267:473–82.

Immunogenetics (2013) 65:107–114
DOI 10.1007/s00251-012-0663-8

ORIGINAL PAPER

MxA transcripts with distinct first exons and modulation of gene expression levels by single-nucleotide polymorphisms in human bronchial epithelial cells

Satoshi Noguchi · Minako Hijikata · Emi Hamano · Ikumi Matsushita · Hideyuki Ito · Jun Ohashi · Takahide Nagase · Naoto Keicho

Received: 3 September 2012 / Accepted: 22 October 2012 / Published online: 18 November 2012

Abstract Myxovirus resistance A (MxA) is a major interferon (IFN)-inducible antiviral protein. Promoter single-nucleotide polymorphisms (SNPs) of MxA near the IFN-stimulated response element (ISRE) have been frequently associated with various viral diseases, including emerging respiratory infections. We investigated the expression profile of MxA transcripts with distinct first exons in human bronchial epithelial cells. For primary culture, the bronchial epithelium was isolated from lung tissues with different genotypes, and total RNA was subjected to real-time reverse transcription polymerase chain reaction. The previously reported MxA transcript (T1) and a recently registered transcript with a distinct 5′ first exon (T0) were identified. IFN-β and polyinosinic–polycytidylic acid induced approximately 100-fold higher expression of the T1 transcript than that of the T0 transcript, which also had a potential ISRE motif near its transcription start site. Even without inducers, the T1 transcript accounted for approximately two thirds of the total expression of MxA, levels of which were significantly associated with its promoter and exon 1 SNPs (rs17000900, rs2071430, and rs464138). Our results suggest that MxA observed in respiratory viral infections is possibly dominated by the T1 transcript and partly influenced by relevant 5′ SNPs.

Keywords Myxovirus resistance A · Single-nucleotide polymorphism · Human bronchial epithelial cells · Transcript variants

Abbreviations

LD	Linkage disequilibrium
HBE	Human bronchial epithelial
ISRE	Interferon-stimulated response element

Introduction

The interferon (IFN) system plays an important role in innate immunity against pathogens. When viral components are detected by pattern recognition receptors, infected cells produce type I (α and β) and type III (λ) IFNs (Randall and Goodbourn 2008). Binding of IFNs to their specific receptors leads to the induction of more than 300 IFN-stimulated genes, including myxovirus resistance A (MxA), also known as the myxovirus (influenza virus) resistance 1, IFN-inducible protein p78 (mouse) (MX1) gene. Following

Electronic supplementary material The online version of this article (doi:10.1007/s00251-012-0663-8) contains supplementary material, which is available to authorized users.

S. Noguchi · M. Hijikata · E. Hamano · I. Matsushita · N. Keicho (✉)
Department of Respiratory Diseases, Research Institute, National Center for Global Health and Medicine, 1-21-1 Toyama, Shinjuku-ku, Tokyo 162-8655, Japan
e-mail: nkeicho-tky@umin.ac.jp

S. Noguchi · E. Hamano · T. Nagase
Department of Respiratory Medicine, University of Tokyo Hospital, Tokyo 113-0033, Japan

H. Ito
Department of Thoracic Surgery, National Center for Global Health and Medicine, Tokyo 162-8655, Japan

J. Ohashi
Molecular and Genetic Epidemiology, Faculty of Medicine, University of Tsukuba, Ibaraki 305-8575, Japan

IFN-induced expression, MxA is thought to form oligomeric rings around the nucleocapsid structures of viruses, thereby inhibiting their transcriptional and replicative functions (Haller and Kochs 2011).

The promoter of the human MxA transcript in the original report contains two IFN-stimulated response elements (ISRE), ISRE1 and ISRE2, near the transcription start site, and both are involved in IFN responsiveness (Ronni et al. 1998). The IFN-stimulated gene factor 3 complex binds to the most proximal ISRE1 and the second ISRE2. ISRE1 is essential for MxA promoter activation, whereas ISRE2 has an enhancing effect in the presence of activated ISRE1 (Ronni et al. 1998). IFN regulatory factor 3 can only bind to ISRE2 for enhancing promoter activation (Holzinger et al. 2007). Around ISRE2, there are two single-nucleotide polymorphisms (SNPs) at nucleotide positions −88 and −123, which confer differences in the promoter activity and binding affinity to nuclear proteins (Hijikata et al. 2001; Ching et al. 2010). Promoter SNPs of MxA are reportedly associated with diseases, including hepatitis C (Hijikata et al. 2000; Hijikata et al. 2001), hepatitis B (Peng et al. 2007), multiple sclerosis (Furuyama et al. 2006), and subacute sclerosing panencephalitis (Torisu et al. 2004). We previously reported the association of MxA promoter SNP with the severity of severe acute respiratory syndrome (SARS; Hamano et al. 2005), and Ching et al. (2010) reported its association with susceptibility to SARS in a larger case–control study. However, the expression levels of MxA have been analyzed only in peripheral blood mononuclear cells (PBMC) or liver cells (Fernandez-Arcas et al. 2004; Kong et al. 2007; Abe et al. 2011; McGilvray et al. 2012).

Because MxA has a pivotal role in host defense against not only SARS coronavirus but also other respiratory viruses such as influenza virus (Haller and Kochs 2011), it is important to characterize the expression profile of MxA in human bronchial epithelial (HBE) cells, a site for replication of many respiratory viruses. In addition, a new transcript variant with alternative 5′ untranslated exons starting 5.5 kb upstream of the original exon 1 has recently been registered in the public database (NM_001144925.1). In the present study, we analyzed the expression patterns of MxA transcripts with distinct first exons. We further investigated the possible effects of their 5′ SNPs on gene expression levels in a panel of primary cultured HBE cells with different genotypes.

Materials and methods

Cell culture

The study protocol was approved by the ethical committee of the National Center for Global Health and Medicine (formerly, International Medical Center of Japan). Primary cultured HBE cells were obtained from the cancer-free bronchi of surgically resected lungs after obtaining written informed consent from the individuals concerned, all of whom were Japanese. HBE cells (n=38) were isolated and cultured as described previously (Gray et al. 1996) and used after three–five passages in this study. In brief, HBE cells were seeded at a density of 5×10^5/well onto collagen-coated six-well Transwell plates (Corning Inc., Corning, NY, USA) and cultured in bronchial epithelial growth medium (Bio-Whittaker, Walkersville, MD, USA) for 24 h. Thereafter, HBE cells (n=3) were stimulated with 1,000 IU/ml IFN-α (PeproTech EC Ltd., London W6 8LL, UK), 1,000 IU/ml IFN-β (Biosource International, Camarillo, CA, USA), 100 μg/ml polyinosinic–polycytidylic acid [poly(I:C); Sigma-Aldrich, St. Louis, MO, USA], 10 ng/ml IFN-γ (R&D Systems, Minneapolis, MN, USA), 50 ng/ml TNF-α (R&D Systems), 20 μg/ml lipopolysaccharide (LPS; Sigma-Aldrich), 10 μg/ml α-defensin 1 (Peptide Institute Inc., Osaka, Japan), 10 μg/ml β-defensin 1 (Peptide Institute Inc.), and 10 μg/ml β-defensin 2 (Peptide Institute Inc.) for 24 h and then harvested. Unstimulated HBE cells (n=38) and those stimulated with 100 μg/ml poly(I:C) for 24 h (n=29) or with 1,000 IU/ml IFN-β for 12 h (n=9) were harvested, and gene expression levels were then analyzed. To assess time-dependent changes in mRNA expression, BEAS-2B cells (ATCC number CRL-9609) were stimulated with 100 μg/ml poly(I:C) for 6, 12, 24, and 48 h.

Real-time reverse transcription polymerase chain reaction

We designated the MxA transcript originally reported by Horisberger et al. (1990) (NM_002462.3) as the T1 transcript and the new transcript variant in the public database (NM_001144925.1) as the T0 transcript. Distinct exons used in the T0 transcript are shown as exons 0a, 0b, and 0c (Fig. 1). Translational start codons of both the T1 and T0 transcripts originate from exon 5, indicating that exons 0a–0c and exons 1–4 are all 5′ untranslated exons.

Total RNA of the cells was extracted using the RNeasy Mini Kit (Qiagen, Hamburg, Germany). Human Total RNA Master panel II (Clontech, Mountain View, CA, USA) was used to investigate gene expression in various tissue types. Most of the tissue RNA in this panel consisted of pooled RNA from two or more donors, and their genotypes were not available. One microgram of total RNA was subjected to RT with random nonamers using SuperScript III Reverse Transcriptase (Invitrogen, Carlsbad, CA, USA). MxA mRNA expression was analyzed by real-time reverse transcription polymerase chain reaction (RT-PCR) using SYBR Premix Ex Taq (Takara Bio, Shiga, Japan) and CFX96 (BioRad, Hercules, CA, USA). Sense and antisense primers were located in exons 0b and 0c (5′-CCAGAGCAACTCCACACCGGGTGC-3′ and 5′-GCTATGGTTCCAATCCAGGTGATC-3′) for the T0 transcript and exons 1 and 2

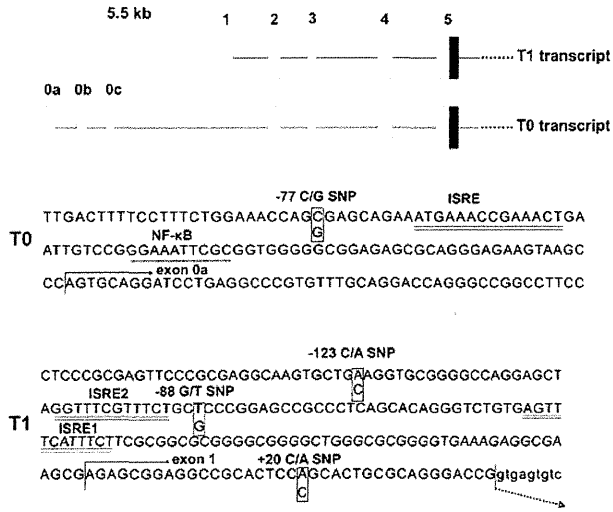

Fig. 1 Alternate splicing of 5′ exons in MxA. The 5′ genomic structure of MxA and nucleotide sequences around the transcription start sites of the T0 and T1 transcripts are shown. *White boxes* represent the untranslated mRNA sequence, and *black boxes* represent the translated sequence. Potential ISREs are *double underlined*, NF-κB binding site is *underlined*, and promoter and exon 1 SNPs are *boxed*. The transcription start site (Horisberger et al. 1990) and nucleotide positions shown in the T1 transcript are displayed in accordance with MxA promoter analysis by Ronni et al. (1998)

(5′-GCACTGCGCAGGGACCG-3′ and 5′-TGGG-TGAG-CAGGTGGGCGGCA-3′) for the T1 transcript. PCR conditions consisted of 40 cycles of denaturation for 15 s at 95 °C and annealing and extension for 1 min at 60 °C. Specific target amplification was confirmed by a single peak in the dissociation curve. The mRNA copy numbers between different transcripts were compared using the absolute quantification method (Leong et al. 2007). RT-PCR products were purified using the Wizard PCR Preps DNA Purification System (Promega, Fitchburg, WI, USA), and their copy numbers were calculated from the DNA concentration determined by measuring the absorbance at 260 nm. The standard curve was generated with a serial fivefold dilution of each RT-PCR product, and the linear dependence of the threshold cycles was confirmed from the template concentrations. We used the β-actin gene (primers listed in Online Resource 1) to normalize the expression of MxA for calculating the relative amounts of mRNA of each transcript. The TaqMan Gene Expression Assay (Hs00182073_m1) (Applied Biosystems, Foster City, CA, USA) that amplifies exons 16–17 of MxA was used with TaqMan Universal Master Mix II (Applied Biosystems) in the StepOne Plus Real-Time PCR System (Applied Biosystems), and the relative amount of total transcripts, indicating the overall expression of MxA, was calculated using the standard curve method with glyceraldehyde 3-phosphate dehydrogenase as an internal control.

Rapid amplification of 5′ cDNA end

RNA ligase-mediated rapid amplification of 5′ cDNA end (5′ RACE) was performed using total RNA from IFN-β-stimulated HBE cells to determine the transcription start site of T0 using the First-Choice RLM-RACE Kit (Ambion, Austin, TX, USA). Gene-specific primers are listed in Online Resource 1. PCR products were sequenced with the BigDye Terminator v3.1 Cycle Sequencing Kit (Applied Biosystems) using a 3130xl Genetic Analyzer (Applied Biosystems).

Screening and genotyping of polymorphisms in the 5′ region

Genomic DNA was extracted from HBE cells (n=38) using the QIAamp DNA Mini Kit (Qiagen). The 5′ upstream region of the transcription start site for the T0 transcript was amplified with two overlapping PCR products, and the amplified products were sequenced using appropriate inner primers. Three SNPs, −123 C/A (rs17000900), −88 G/T (rs2071430), and +20 C/A (rs464138), two in the promoter and one in exon 1 of the T1 transcript, were genotyped by PCR and restriction fragment length polymorphism methods (Hamano et al. 2005), with Pst I (Takara Bio) for rs17000900, Hha I (Takara Bio) for rs2071430, and Bpm I (New England Biolabs, Ipswich, MA, USA) for rs464138. The primers are listed in Online Resource 1. Linkage disequilibrium (LD) between promoter SNPs was analyzed using Haploview (v. 4.2) (Barrett et al. 2005).

Statistical analysis

All data were expressed as mean±standard error of the mean (SEM). To assess the relationship between the number of single alleles of −123 C/A, −88 G/T, and +20 C/A SNPs and expression levels of the transcript variants, a simple linear regression model was applied (JMP, version 9.0.0; SAS Institute Inc., Cary, NC, USA). A multiple linear regression model was also applied to assess the combined effects of these SNPs on expression of the T1 transcript. The numbers of alleles of the three abovementioned SNPs were incorporated in the model as explanatory variables. Correlations of the total amount of the MxA transcripts with expression levels of the T0 and T1 transcripts were further analyzed using Spearman's rank correlation coefficient. A p value <0.05 was considered to be statistically significant.

Results

Expression patterns of MxA transcripts in human tissues

The originally reported MxA transcript, T1, and a recently registered transcript variant, T0, were both successfully

amplified by RT-PCR from various human tissues (Fig. 2). Expression of the T1 transcript was predominant in the tissues examined, including the lung and trachea, whereas expression of the T0 transcript was inconspicuous, except in the testis and adrenal gland.

Induction patterns of MxA transcripts in HBE cells incubated with type I IFNs and other stimuli

MxA transcripts, T0 and T1, were both detected in the unstimulated primary cultured HBE cells (n=3), and their expression was markedly induced by type I IFNs and poly(I:C), although induction of the T1 transcript was much stronger than that of the T0 transcript (Fig. 3). IFN-γ, TNF-α, and α-defensin 1 also induced expression of the T1 transcript to a lesser extent, whereas this increase was not observed in the T0 transcript.

Genomic structure and genetic polymorphisms in the 5′ upstream regions of MxA transcripts with distinct first exons

Because the transcript variant T0 with alternatively spliced exons was moderately induced by type I IFNs, 5′ RACE was performed to determine the 5′ end of exon 0a, the transcription start site of T0, in IFN-β-stimulated HBE cells (Fig. 1). A putative ISRE motif and a possible binding site for NF-κB were revealed in the 5′ upstream region of the T0 transcript (Fig. 1). The nearly full-length transcript T0 was amplified with the sense primer in exon 0c and the antisense primer in the last exon 17; however, no alternatively spliced exon was observed in the protein-coding region (data not shown). Although the transcript variant that skips untranslated exons 2

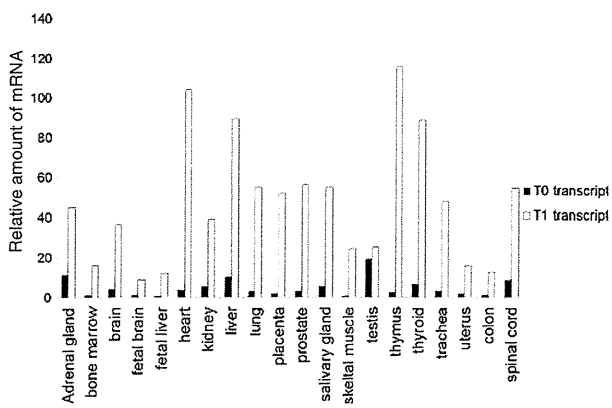

Fig. 2 Relative expression levels of two MxA transcript variants in human tissues. Relative expression levels of the T0 and T1 transcripts in various human tissues were obtained by real-time RT-PCR using a commercial RNA panel, Human Total RNA Master panel II (Clontech). The RNA consisted of pooled RNA from two or more donors. Their genotypes were not available but presumably mixture of different genotypes

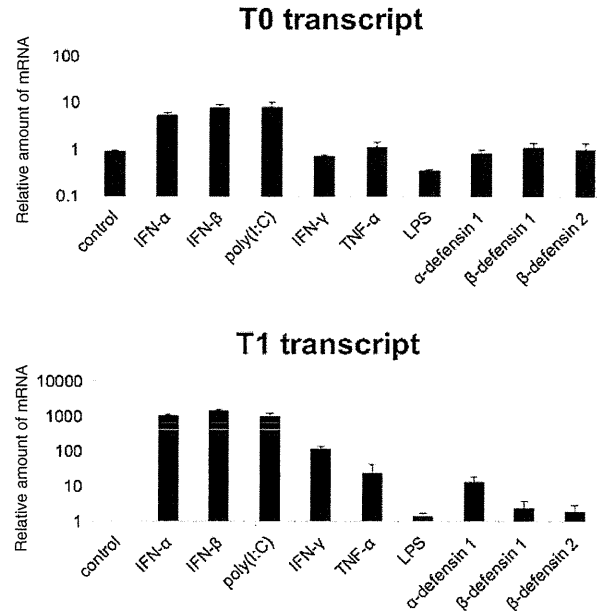

Fig. 3 Induction of T0 and T1 transcript variants by various stimuli in HBE cells. HBE cells (n=3) were stimulated with IFN-α, IFN-β, poly (I:C), IFN-γ, TNF-α, LPS, α-defensin 1, β-defensin 1, and β-defensin 2 for 24 h and then harvested. Expression levels of the T0 and T1 transcripts were compared with those of unstimulated cells by real-time RT-PCR. Fold inductions are shown as the mean±SEM. The genotypes of the promoter SNPs were as follows: sample #1, −77 SNP (rs457274) C/G, −123 SNP (rs17000900) C/A, −88 SNP (rs2071430) G/T, and +20 SNP (rs464138) C/A; sample #2, −77 C/C, −123 C/A, −88 T/T, and +20 A/A and; sample #3, −77 C/G, −123 C/C, −88 G/G, and +20 C/A

and 4 has also been registered in the public database (NM_001178046.1), its expression level was very low in the HBE cells (data not shown).

Sequence analysis of the 5′ upstream region of the T0 transcript using our DNA samples identified genomic variations, −77 C/G SNP (rs457274) near the putative ISRE motif (Fig. 1), −326 deletion/insertion polymorphism (rs60467231), and −504 A/G SNP (rs12483338). Three other SNPs, −123 C/A (rs17000900), −88 G/T (rs2071430), and +20 C/A (rs464138), near the 5′ end of the T1 transcript were also detected (Fig. 1). As shown in Online Resource 2, −77 C/G SNP of the T0 transcript and the three SNPs near the 5′ end of the T1 transcript were all in strong LD with each other (D'> 0.8, r^2>0.4).

Differences in expression levels of MxA among SNP genotypes

Next, the mRNA expression levels of the T0 and T1 transcripts were analyzed in HBE cells with different genotypes. The expression of the T1 transcript assessed by real-time RT-PCR was 2.3-fold higher than that of the T0 transcript under the unstimulated condition (n=38). Baseline expression of the T1 transcript was significantly higher in proportion to the

number of A alleles of −123 C/A SNP, T alleles of −88 G/T SNP, and A alleles of +20 C/A SNP carried by HBE cells according to a simple regression analysis (p=0.013, p=0.0035, and p<0.0001, respectively) (Fig. 4b). Multiple regression analysis showed that the association of +20 C/A SNP remained significant (p=0.016), whereas the association of −123 C/A and −88 G/T SNPs was insignificant (p=0.67 and p=0.78, respectively). In contrast, baseline expression of the T0 transcript was slightly higher in proportion to the number of C alleles of −77 C/G SNP; however, this increase was not statistically significant (p=0.086) (Fig. 4a).

When the relative expression of the total MxA transcripts was compared with expression of the T1 and T0 transcripts under the unstimulated condition, the overall expression of MxA strongly correlated with expression of the T1 transcript (Spearman's rank correlation coefficient; rs=0.759), whereas it weakly correlated with expression of the T0 transcript (rs=0.388). The total expression of MxA was significantly higher in proportion to the number of −123 A, −88 T, and +20 A alleles (p=0.0004, p<0.0001, and p< 0.0001, respectively), which was similar to the linear relationship between the T1 transcript and number of alleles shown above.

When immortalized HBE cell line BEAS-2B was stimulated with poly(I:C), time-course analysis revealed that expression of the T0 transcript was the highest after 24 h, whereas that of the T1 transcript was the highest after 6–12 h of incubation (Online Resource 3). We therefore investigated the expression of T0 and T1 transcripts in HBE cells (n=29) stimulated with poly(I:C) for 24 h. The expression of the T0 transcript increased eightfold, whereas that of the T1 transcript increased 870-fold. Poly(I:C)-induced expression of both transcripts was not associated with either allele of the four SNPs (Fig. 5a, b). When HBE cells (n=9) were stimulated with IFN-β for 12 h, the T0 transcript was induced eightfold, and the T1 transcript was induced 640-fold. IFN-β-induced expression of the transcripts did not vary among genotypes (data not shown).

Discussion

In this study, we investigated the expression profile of MxA by analyzing expression of the original transcript T1 and the transcript variant T0 in primary cultured HBE cells. According to our absolute quantification method using real-time RT-PCR, the amount of the T0 transcript was approximately half of that of the T1 transcript at the baseline level. Although expression of the T0 transcript was also induced by type I IFNs and poly(I:C) and its 5′ proximal region has a potential ISRE motif, IFN-β and poly(I:C) inducibility of the T1 transcript was at least 100-fold higher than that of the

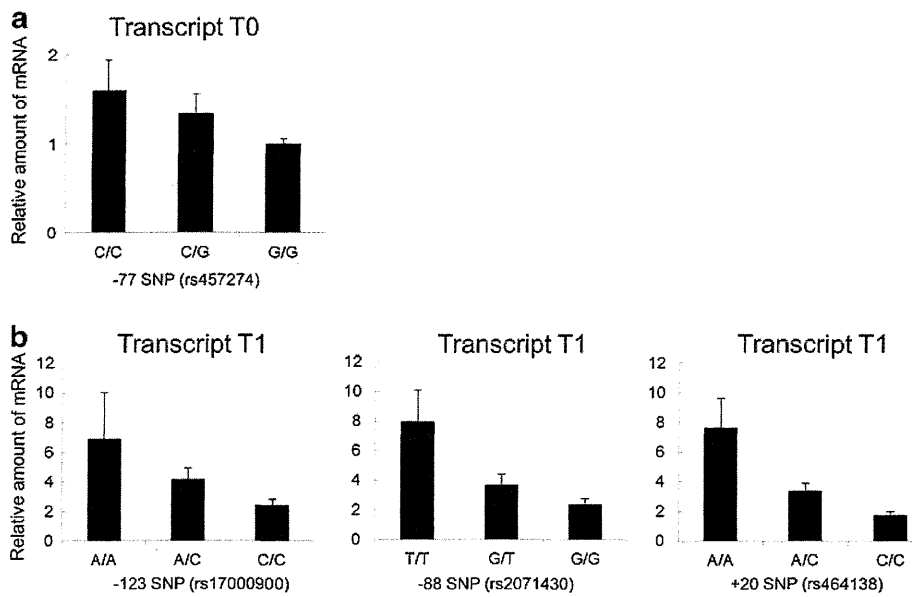

Fig. 4 Differences in the baseline expression of transcript variants among the genotypes of the promoter and exon 1 SNPs in HBE cells. Expression of **a** T0 and **b** T1 transcripts under the unstimulated condition in HBE cells with each genotype of −77 C/G SNP for the T0 transcript (C/C, n=8; C/G, n=18; G/G, n=12), of −123 C/A SNP (A/A, n=2; A/C, n=18; C/C, n=18), of −88 G/T SNP (T/T, n=3; G/T, n=19; G/G, n=16), and of +20 C/A SNP (A/A, n=5; A/C, n=22; C/C, n=11) for the T1 transcript is shown. The relative amounts of mRNA of each transcript compared with that of the T0 transcript in GG cells without poly(I:C) stimulation are shown as mean±SEM. Possible associations between the number of alleles and the amount of the corresponding transcripts were assessed by a simple regression model respectively (p=0.086 for the number of −77 C alleles, p=0.013 for −123 A alleles, p=0.0035 for −88 T alleles, and p<0.0001 for +20 A alleles)